Aus dem Medizinischen Zentrum für Operative Medizin
Klinik für Urologie und Kinderurologie
Geschäftsführender Direktor: Prof. Dr. Rainer Hofmann

des Fachbereichs Medizin der Philipps-Universität Marburg

Expression und Funktion des Tumor Antigens MAGE-A3 an Zelllinien des Harnblasenkarzinoms

Expression and function of the tumor antigen MAGE-A3 in bladder cancer cell lines

Inaugural-Dissertation
Zur
Erlangung des Doktorgrades der gesamten Humanmedizin
dem Fachbereich Medizin der Philipps-Universität Marburg
vorgelegt von

Gaofeng Zhou

aus Hunan, China

Marburg, 2020

Angenommen vom Fachbereich Medizin der Philipps-Universität

Marburg am: 27.07.2020

Gedruckt mit Genehmigung des Fachbereichs

Dekan: **Prof. Dr. H. Schäfer**

Referent: **PD Dr. J. Hänze**

Korreferent: **PD Dr. S. Müller-Brüsselbach**

I. Table of content

I. Table of content

Ⅱ. List of figures and tables

List of figures

List of tables

III. Abbreviations

ASCIs	Antigen-specific cancer immunotherapeutics
ATCC	American Type Culture Collection
BSA	Bovine serum albumin
BCA	Bicinchoninic acid
°C	Celsius
cDNA	Complementary deoxyribonucleic acid
CLS	Cell Line Service
CO2	Carbon dioxide
CTA	Cancer/testis antigens
CTL	Cytotoxic T lymphocyte
DMSO	Dimethylsulfoxide
DSMZ	Leibniz institute DSMZ-German collection of microorganisms and cell cultures
dNTP	Deoxyribose nucleotide triphosphate
DNA	Deoxyribonucleic acid
ECL	Enhanced Chemi Luminescence
FCS	Fetal calf serum
HRP	Horseradish peroxidase
HEPES	4-(2-hydroxyethyl)-1-piperazineethanesulfonic acid
Kb	Kilo base
kDa	Kilo dalton
MAGE	Melanoma-associated antigen
MHD	MAGE homology domain
mm	Millimetre
mM	millimolar
min	Minute
ml	Milliliter
mRNA	Messenger RNA

M-MuLV	Moloney murine leukemia virus
NaCl	Sodium chloride
nM	nanomolar
p21	protein 21
p53	protein 53
PBS	Phosphate buffer saline
PCR	Polymerase chain reaction
pmol	picomole
RT-PCR	Reverse transcription-PCR
RNA	Ribonucleic acid
Rnase	Ribonuclease
RPMI	Roswell park memorial institute
RT	Room temperature
si-RNA	Small interfering RNA
s	Second
TCC	transitional cell carcinoma
Tris	Tris-(hydroxy methyl)-amino methane
TBST	Tris-Buffered Saline and Tween 20
V	Volt
V/V	Volume to volume
XTT	2,3-Bis(2-methoxy-4-nitro-5-ulfophenyl)-2H-tetrazolium-5-carbox-anilide
µl	microlitre
µM	micromolar
µm	micrometer

1.Introduction

1.1 Phylogeny of melanoma-associated antigen (MAGE) family

In 1991, the first melanoma-associated antigen gene was identified by Terry Boon and his colleagues (Simpson *et al.*, 2005; Traversari *et al.*, 1992b; van der Bruggen *et al.*, 1991) in a melanoma patient. The identification of this MAGE gene was due to its processing and expression as a peptide bound to major histocompatibility complexes on the cell surface (Herin *et al.*, 1987; Traversari *et al.*, 1992a; van der Bruggen *et al.*, 1991). This gene was later renamed MAGE-A1 because it was found to belong to a 12-hMAGE-A genes cluster (Chomez *et al.*, 2001). The family of MAGE genes has undergone expansion during the past years and now consists of approximately 60 identified members that are still under experimental investigation (Chomez *et al.*, 2001). The functional role of most MAGE family members remains to be characterized. Recent studies are beginning to provide insights into MAGE gene functions and their potential for cancer immunotherapy.

1.2 Classification of MAGE family

Based on their different expression patterns, chromosomal locations, and gene structures, the MAGE family has been divided into two subfamilies: type I cancer-testis antigens (CTA) and type II omnipresent MAGEs.

Type I MAGE genes are located in clusters of the X chromosome and rarely expressed in normal adult tissues except testis, trophoblast, and placenta (Barker and Salehi, 2002; Simpson *et al.*, 2005), but have high expressions in various cancers. These genes have been classified as type I MAGE genes which belong to CTA due to their special expression pattern, genomic clustering, and single exon open reading frame. Type I MAGE genes consist of MAGE-A, -B, and -C groups according to chromosomal localization (Lucas *et al.*, 1998; Muscatelli *et al.*, 1995; Rogner *et al.*,

1995). MAGE-A, -B, and -C genes locate in the q28, p21-22 and q26-27 regions of the X chromosome, respectively (Dabovic *et al.*, 1995; De Plaen *et al.*, 1994; Lucas *et al.*, 2000; Lucas *et al.*, 1998; Lurquin *et al.*, 1997; Muscatelli *et al.*, 1995; Rogner *et al.*, 1995) (Figure 1).

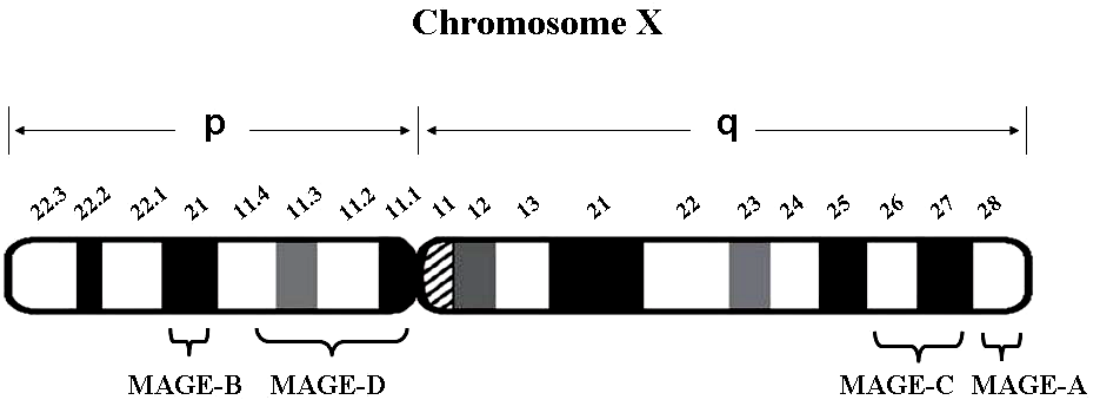

Figure 1: Chromosomal locations of the human MAGE genes
*Figure modified from Sang et al.(Sang *et al.*, 2011b).

Type II MAGE gene family consist of 15 genes and their genomic locations are not limited to the X chromosome. They are broadly expressed in a variety of normal adult tissues (Ohman Forslund and Nordqvist, 2001) and not specifically related to cancer (De Plaen *et al.*, 1999; Osterlund *et al.*, 2000; Sang *et al.*, 2011b). Furthermore, type II MAGE genes are related to many biologic processes, such as cell cycle withdrawal, neuronal differentiation and programmed cell death (Barker and Salehi, 2002; Espantman and O'Shea, 2010).

1.3 Structure of MAGE

MAGE genes belong to a large gene family and all members have a conserved 165-171 amino acid domain in the center of the molecule (Figure 2) named MAGE homology domain (MHD) (Chomez *et al.*, 2001; Lopez-Sanchez *et al.*, 2007).

Human MHDs consist of 165-171 amino acids and can be divided into five different regions which represent distinct areas of conservation (Barker and Salehi, 2002). It

has been shown that the MHD contains at least four potential α-helical domains and five regions of α-sheet structure according to the structural predictions. Additionally, a single MHD flanked by a small amount of poorly conserved N- and C-terminal sequence exists in most of type I MAGE genes. Type II MAGE family members can be divided into two groups: one group includes Necdin, MAGE-F1, and MAGE-G1 whose structures are similar to MAGE-A and -B genes; the other group are larger proteins with extended N- or C-termini including MAGE-D1-4, MAGE-E1, and MAGE-L2 (Figure 2B).

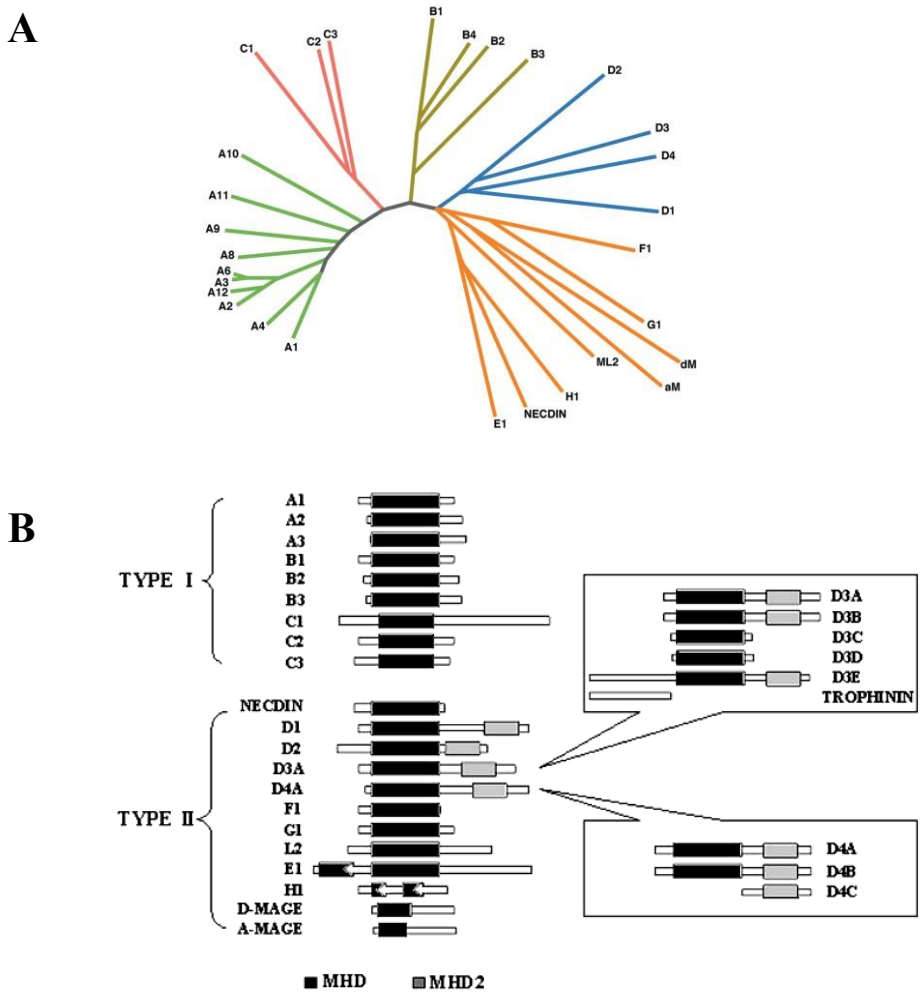

Figure 2: The phylogeny and structure of MAGE family members

A: An evolutionary tree using the aligned MHDs shows the relationship of MAGE family members. **B:** Domain structures of selected MAGE family members are shown. MHD: MAGE homology domain. MHD2: a loosely conserved region located in the N-terminal domain of some type II MAGE genes. The presence of truncated MHDs was indicated by the notched lines in the MHDs of MAGE-E1 and MAGE-H1.

*Figure modified from Barker PA et al.(Barker and Salehi, 2002).

1.4 Expression of MAGE

It has been described previously that type I MAGE genes are normally restricted in their expression to the testis, trophoblast, and placenta. It also has been shown that aberrant type I MAGE expressions could be detected in various human cancers, including melanoma, lung cancer, breast cancer, oral squamous cell carcinoma, esophageal carcinoma, urothelial malignancies, hematopoietic malignancies, etc. (Bergeron *et al.*, 2009; Brasseur *et al.*, 1995; Jang *et al.*, 2001; Lin *et al.*, 2004; Otte *et al.*, 2001; Ries *et al.*, 2009; Suyama *et al.*, 2002).

Among various cancers, melanoma and lung cancer have the highest frequency of type I MAGE gene expression. It was reported that the frequencies of MAGE-A1, A3 and C1 gene expression in melanoma specimens were 36%, 69% and 46%, respectively (Gaugler *et al.*, 1994; Itoh *et al.*, 1996; Lucas *et al.*, 1998). MAGE-A3 gene was expressed in 76% of metastatic melanoma cases (Ohman Forslund and Nordqvist, 2001). It was also shown that MAGE-B1 and B2 gene had very high expression in lung cancer and melanoma (De Smet *et al.*, 1999). The frequency of MAGE-I mRNA expression was found to be intermediate in other epithelial cancers, such as breast cancer, prostate cancer and bladder cancer. But the frequency of MAGE-I mRNA expression is extremely low in renal cancer, colon cancer, pancreatic cancer and hematopoietic malignancies including lymphomas and leukemia.

At present, most studies demonstrated that the expression of type I MAGE gene was closely related to the staging, metastasis and recurrence of malignant tumors (Kufer *et al.*, 2002; Mou *et al.*, 2002; Taback *et al.*, 2001). However, there are still a lot of disputations on the relationship between type I MAGE gene expression and the occurrence and development of malignant tumors.

Type II MAGE genes differ greatly from type I MAGE genes in expression. Type II MAGE genes are not limited to germline expression and can be broadly expressed in a variety of normal adult tissues. Only several type II MAGE genes, such as necdin

and MGAE-E1, are highly expressed in various forms of cancer (Masuda *et al.*, 2001; Muscatelli *et al.*, 2000; Niinobe *et al.*, 2000; Ohman Forslund and Nordqvist, 2001; Salehi *et al.*, 2000; Sasaki *et al.*, 2001).

1.5 Function of MAGE

Although MAGE genes were identified twenty years ago, their possible biological functions on cellular transformation or tumor progression are largely unknown. But studies from diverse areas now suggested that they might be involved in the regulation of cell survival, cell cycle progression, and cell apoptosis.

Some evidences have been reported that MAGE-A antigens may have some important effects in human tumors. Overexpression of MAGE-A11 was found to promote transcriptional activity of androgen receptor (AR) and thus promote the progression of prostate cancer (Askew *et al.*, 2010; Askew *et al.*, 2009; Bai *et al.*, 2005; Bai and Wilson, 2008). Additionally, Overexpression of MAGE-A11 markedly promoted breast cancer cell proliferation and the capacity of producing colonies (Xia *et al.*, 2012). Down-regulation of MAGE-A3 was shown to induce apoptosis or reduce cell survival in various cell lines through different mechanism (Nardiello *et al.*, 2011; Yang *et al.*, 2007; Zhu *et al.*, 2008). MAGE-A1 was found to function as a transcriptional inhibitor by binding to Ski interacting protein and by recruiting histone deacetylase 1 (Laduron *et al.*, 2004). Furthermore, some MAGE-A proteins including MAGE-A1, -A2, -A3, and -A6 are able to suppress p53 transactivation function which result in the resistance to anti-tumor drugs (Monte *et al.*, 2006). Recently, it was identified that some MAGE proteins such as a sub-family E3 ubiquitin ligases were able to interact with RING domain proteins, thus promoting the ubiquitylation and the subsequent p53 degradation (Doyle *et al.*, 2010; Espantman and O'Shea, 2010; Feng *et al.*, 2011; Zendman *et al.*, 2003). These data suggest that MAGE-A proteins may function as oncoproteins inhibiting cell apoptosis and promoting cell proliferation so that they facilitate the development of malignancies.

However, MAGE-A4 is a untypical member among the MAGE-A family. A retrospective study showed that patients with MAGE-A4 expression survived significantly longer than MAGE-A4-negative patients (Bandic *et al.*, 2006). MAGE-A4 was found to induce apoptosis when it was overexpressed in human cells (Peikert *et al.*, 2006; Sakurai *et al.*, 2004). Furthermore, it was shown that MAGE-A4 could bind to Gankyrin which has been implicated in the formation of hepatocellular carcinoma and inhibited Gankyrin-mediated carcinogenesis (Nagao *et al.*, 2003). Therefore, MAGE-A4 was considered as an anti-oncogenic protein in malignancies.

Some MAGE II proteins such as Necdin, MAGE-D1 and MAGE-D4 have been involved in cell proliferation and apoptosis according to recent studies. Necdin was found to interact with E2F1 and p53 thus inhibiting cell growth and apoptosis (Taniura *et al.*, 1999; Taniura *et al.*, 1998). MAGE-D1 was found to inhibit cell cycle progression and induce apoptosis which depends on nerve growth factor through interacting with p75 neurotrophin receptor and inhibitor of apoptosis proteins (IAP) (Jordan *et al.*, 2001; Salehi *et al.*, 2000). Moreover, overexpression of MAGE-D4B exhibited an increase of cell growth and promoted migration in oral squamous cancer (Chong *et al.*, 2012).

In sum, the known biological functions of MAGEs in different cells can be quite heterogenous.

1.6 Type I MAGE antigens and tumor specific immune therapy

For developing antigen-specific cancer immunotherapy, the most crucial step is to discover rational target antigens which must have no or highly restricted expression in normal tissues so that the autoimmunity can be avoided. Type I MAGE antigens have gained extensive attention on the development of effective anticancer immunotherapies in recent years due to their tumor-specific expression. It has to be mentioned that testis which expresses MAGE-I is regarded as an immunoprivileged organ and can escape from autoimmune response.

Type I MAGE antigens are the best studied CTA, particularly the MAGE-A subcategory. MAGE-A antigens are one of the most appropriate target antigens for immunotherapy because they are strictly tumor specific and are expressed in a large variety of tumors. Graff-Dubois's study showed that several heteroclitic peptides such as p248V9, p248G9 and p248D9, derived from MAGE-A1, -A2, -A3, -A4, -A6, -A10 and MAGE-A12, were able to stimulate cytotoxic T lymphocytes which could recognize each MAGE-A antigen individually and lead to tumor cells destruction (Graff-Dubois *et al.*, 2002).

Dozens of clinical studies of therapeutic vaccination targeting these antigens have been performed, particularly MAGE-A3. There are two large phase III clinical trials which have been initiated in patients with melanoma skin cancer and non-small cell lung cancer, using MAGE-A3 as an adjuvant immunotherapy (Russo *et al.*, 2011; Tyagi and Mirakhur, 2009). The studies will also evaluate potential side effects of MAGE-A3 ASCIs (Antigen-specific cancer immuno-therapeutics).

1.7 Tumor specific immune therapy for bladder cancer

Bladder cancer is a worldwide health problem with an age-standardised incidence rate (per 100000 persons) of 17.7 for males and 3.5 for females in Europe. 95% of bladder cancers are defined as transitional cell carcinoma (TCC) (Patton *et al.*, 2002), and 75% of them are superficial (Amling, 2001). Most TCCs are likely to recur after treatment and a significant proportion (5%–25%) of the recurrences will progress to a more aggressive stage. It has been shown that superficial bladder cancer effectively responds to nonspecific immunotherapy with Bacillus Calmette-Guerin (BCG) by using intravesical treatment, especially carcinoma *in situ* disease. This treatment is partially succesful to prevent recurrence and progression of bladder cancer after surgery (Nseyo and Lamm, 1997). Based on this finding, development of immunotherapeutic approaches targeting MAGE are suggested for treatment of bladder cancer. Therefore, MAGEs are under investigation as possible targets for

bladder cancer immunotherapy. In particular, MAGE-A3 is one of the most abundantly expressed MAGE subtype in bladder cancer (Yin *et al.*, 2011) and MAGE-A3 vaccination protocols are investigated in clinical trials. Interestingly, a recent study with recombinant MAGE-A3 combined with local BCG immunostimulation for treatment of non-muscle-invasive bladder cancer increased total and vaccine-specific T-cells in the bladder (Derre *et al.*, 2017). However, so far, the intrinsic functions of MAGE-A3 in bladder cancer cells are not clear and represent the topic of this study.

2. Aims of the study

The type I Melanoma Antigen Genes such as MAGE-A3 are expressed in various cancers including bladder cancer. In normal tissues, MAGE-A3 is restricted to testis and placenta representing tissues with low antigen presentation. Thus, MAGE-A3 represents a candidate antigen as possible target for cancer immunotherapy. In particular, MAGE-A3 vaccination protocols are investigated in clinical trials in bladder cancer. So far, the intrinsic functions of MAGE-A3 in bladder cancer cells are not clear. Different MAGE-A types have been demonstrated to favour or to impede oncogenicity in other cancer types.

This study aimed to analyze whether MAGE-A3 affects oncogenicity in bladder cancer cells. To follow this aim we performed the following strategy:

1. MAGE-A3 expression analysis in bladder cancer cell lines and selection of cell lines for further functional analysis of MAGE-A3.
2. Establishment of silencing of MAGE-A3 by RNA interference with synthetic siRNA.
3. Functional analyses of MAGE-A3 with respect to proliferation, cell viability and apoptosis in bladder cancer cell lines employing silencing of MAGE-A3.
4. Proteomic array analysis of components relevant for proliferation and apoptosis after silencing of MAGE-A3.

3. Materials and methods

3.1 Materials

3.1.1 Cells

Human bladder carcinoma cell lines used in the experiment were purchased from Leibniz Institute DSMZ-German Collection of Microorganisms and Cell Cultures (DSMZ) (T24, 5637, HT-1376 and BFTC-905), American type culture collection (ATCC) (UMUC-3), or Cell Line Service (CLS) (EJ-28).

3.1.2 Oligonucleotides for quantitative RT-PCR

The oligonucleotides were synthesized by Biomers (Biomers, Ulm, Germany)

β-ACTIN

Forward 5′-TATCCAGGCTGTGCTATCCCTGTAC-3′

Reverse 5′-TTCATGAGGTAGTCAGTCAGGTCCC-3′

MAGE-A3

Forward 5′-GAGTCATCATGCCTCTTGAGCAGAG-3′

Reverse 5′-GAGGGTAGTTCATGGTAGTGGGGAG-3′

3.1.3 Small interfering RNA sequences

The oligonucleotides were synthesized by Biomers (Biomers, Ulm, Germany)

Si-MAGE-A3

Forward 5′-GGUAAAGAUCAGUGGAGGA dTdT-3′

Reverse 5′-UCCUCCACUGAUCUUUACC dTdT-3′

Si-Random

Forward 5′- UAGCGACUAAACACAUCAA dTdT -3′

Reverse 5′- UUGAUGUGUUUAGUCGCUA dTdT -3′

3.1.4 Enzymes

DNase I

DNase I (RNase-free) was purchased from Fermentas (Fermentas GmbH, St. Leon-Rot, Germany). DNase I is an endonuclease that nonspecifically cleaves DNA to release di-, tri- and oligonucleotide products with 5′-phosphorylated and 3′-hydroxylated ends. DNase I acts on single- and double-stranded DNA, chromatin and RNA: DNA hybrids. It is frequently used to remove contaminating genomic DNA from RNA samples. (* modified from the product information of Thermo Fisher Scientific Inc.)

RevertAid™ Reverse Transcriptase

RevertAid™ Reverse Transcriptase was purchased from Fermentas (Fermentas GmbH, St. Leon-Rot, Germany). It is a genetically modified M-MuLV RT and differs from wildtype M-MuLV RT by its structure, catalytic properties and in the optimum activity temperature. The enzyme possesses RNA-dependent and DNA-dependent polymerase activity and a RNase H activity specific to RNA in RNA-DNA hybrids. RevertAid™ Reverse Transcriptase activity is optimal at 42°C (active up to 50°C). The enzyme is capable of first strand cDNA synthesis up to 13 kb. The enzyme incorporates modified nucleotides. (* modified from the product information of Thermo Fisher Scientific Inc.)

RiboLock RNase Inhibitor

RiboLock RNase inhibitor was purchased from Fermentas (Fermentas GmbH, St. Leon-Rot, Germany). It inhibits the activity of RNases by binding them in a noncompetitive mode at a 1:1 ratio. It does not inhibit eukaryotic Rnases: T1, T2, U1, U2, CL3, as well as prokaryotic RNases I and H. Its source is *E.coli* cells with a cloned gene encoding mammalian ribonuclease inhibitor with molecular weight of 49.6 kDa monomer. (* modified from the product information of Thermo Fisher Scientific Inc.)

3.1.5 Antibodies

Antibodies used in the experiments are all commercially available. Their parameters were described as follows:

Primary antibodies	**Company**
Anti-human MAGE-A3 (monoclonal) mouse	Proteintech /USA
Link antibody	
Biotinylated rabbit anti-mouse immunoglobulins	Dako, Hamburg, Germany

3.2 Methods

3.2.1 Cell culture of T24, UMUC-3, EJ-28 cells

The cell culture was performed according to the protocols provided by DSMZ, ATCC and CLS. The cells frozen in 10% DMSO in liquid nitrogen (approx. 5 x 10^6 cells/ml) were thawed rapidly at 37°C and then added drop wise to 100 mm dish containing 10ml of pre-warmed RPMI1640 medium (supplemented with 10% (v/v) FCS (fetal calf serum, heat inactivated for 30 min at 56 °C), sterile filtered, 1% (v/v) penicillin and streptomycin, and 1% (v/v) L-glutamine (medium and all supplements were from PAA Laboratories GmbH, Pasching, Austria)). When the cells became confluent, they were trypsinized with 2 ml 1 x trypsin per 100 mm plate for approximate 5 min at 37°C. The reaction was stopped by adding 5 ml of medium with 10% FCS containing trypsin inhibitors. For continuous culture, about 1/4 of the medium containing the cells were transferred to a fresh plate and cultured in a gas controlled incubator (Hera cell, kendro Laboratory Products GmbH, Langenselbold, Germany) with water-saturated atmospheric air and 5% CO2.

1 x Trypsin	Volume
10 x Trypsin	10 ml
HEPES (200 mM)	10 ml
Isotonic NaCl (0.9%)	80 ml

3.2.2 Small interfering RNA preparation and transfection

Selective inhibition of target gene was performed using specific si-RNAs. As a control, si-Random sequence was employed that does not target any gene in the human genome and has been tested by micro-array analysis (Dharmacon Inc., Chicago, IL, USA). The forward and reverse RNA strands with two 5′ deoxy-thymidine overhangs were commercially synthesized and annealed at a final concentration of 20 µM at 37°C for 1h in annealing buffer. The principle of this siRNA technique has been described (Pei and Tuschl, 2006).

RNA duplex annealing buffer	Final concentration
potassium acetate	20 mM
HEPES-KOH	6 mM
magnesium acetate	0.4 mM
pH	7.4

The INTERFERin^{TM} (Polyplus-Transfection, NewYork, USA) mediated transfection method was employed for transfection of T24, UMUC-3 and EJ-28 cells. INTERFERin^{TM} is a powerful siRNA transfection reagent that ensures efficient gene silencing and reproducible transfection. INTERFERin^{TM} delivers efficiently siRNA duplexes to mammalian cells. One day before transfection, appropriate numbers of T24, UMUC-3 and EJ-28 cells were plated on respective culture dishes with growth medium, so that they will become 30-50% confluent at the time of transfection.

Si-RNA duplexes was diluted in medium without serum and mixed gently. INTERFERin™ transfection reagent was added to the diluted si-RNA duplexes and the mixture was homogenized for 10 seconds immediately. The mixture was incubated for 10 minutes at room temperature to form transfection complexes between siRNA duplexes and INTERFERin™. During complex formation, the growth medium was removed and fresh prewarmed complete medium was added to each well. The transfection mix was added onto the cells and then was homogenized by gently swirling the plate. The plate was incubated at 37°C. The medium was replaced with growth medium 6h after transfection. Cells were further incubated according to the experiment need.

Table 1: Protocol for transfection in different plate formats.

Culture format	Volume of si-RNA	Volume of INTERFERin™	Volume of medium without serum for complexe formation	Volume of complete medium on cells	Final volume
96-well	0.23 µl	1.5 µl	50 µl	125 µl	175 µl
6-well	2.5µl	11 µl	200 µl	2 ml	2.2 ml
60 mm	5 µl	22 µl	400 µl	4 ml	4.4 ml
100 mm	12 µl	52.5 µl	500 µl	10 ml	10.5 ml
8-well chamber slide	0.46 µl	3 µl	100 µl	250 µl	350 µl

3.2.3 RNA isolation from cultured cells

Cells were rinsed with PBS, and then were lysed directly in the culture dish by addition of 1 ml TriFast (peqGOLD TriFast, Peqlab Biotechnology GmbH, Erlangen, Germany) to the dish and passing the cell lysate several times through a pipette. The amount of TriFast needed is based on the area of the culture dish (1 ml per 10 cm^2) and not on the number of cells. Then cells were scraped in TriFast and the lysate was

transfered to an appropriate fresh tube. The samples were kept for 5 min at room temperature, then were shaken by hand vigorously after addition of 0.2 ml chloroform per 1 ml TriFast for 15 seconds. The samples were kept for 3-10 minutes at room temperature and then were centrifuged for 10 min at 12,000g (4°C). The mixture was separated into a lower red (phenol-chloroform) phase, an interphase and a colorless upper aqueous phase. RNA was forced exclusively into the aqueous phase and the aqueous phase was transferred to a fresh tube. To precipitate the RNA, 0.5 ml isopropanol per 1 ml of TriFast used for the initial homogenization was added to this tube. Then the tube was shaken and was incubated on ice for 15 min. After that, the tube was centrifuged for 10 min at 12,000g (4°C). The RNA pellet should form a gel like precipitate on the bottom side of the tube. The supernatant was removed carefully and the RNA pellet was washed twice with 75% ethanol by vortexing and subsequent centrifugation for 8 min at 7,500g (4°C). The excessive ethanol was removed from the RNA pellet by air-drying. Later the RNA pellet was resuspended in RNAse-free water. RNA was quantified by spectrophotometer (GeneQuant 1300, GE scientific, UK).

3.2.4 Preparation of cDNA from RNA probes

For the preparation of cDNA, 1 µg RNA per sample was used. RNA was copied to cDNA using reverse transcriptase (RevertAid^{TM} Reverse Transcriptase) and random-hexamer primer (Fermentas). For the negative control, RevertAid^{TM} Reverse Transcriptase was omitted and H_2O (Aqua ad iniectabilia, Braun, Germany) was used instead.

1 µg RNA in H_2O (total volume 10.5 µl) including DNase I was heated up to 37°C for 30 min, 75°C for 5 min, and then cooled down to 4°C. This step is to eliminate DNA. 1µl random-hexamer primer was added to each RNA mixture and the mixture was denatured at 65°C for 5 min followed by rapid cooling and addition of 7.5 µl of the following master mixture:

5 x first strand buffer	4 µl
40 mM dNTP mix (Fermentas)	2 µl
RiboLock RNase Inhibitor	0.5 µl
RevertAid^{TM} Reverse Transcriptase	1 µl (omitted in negtive controll)
H_2O	1 µl (only used in negtive controll)

The denatured RNA mixed with master solution was then subjected to cDNA synthesis by incubating at 25°C for 5 min, 42°C for 60 min followed by inactivation of enzymes at 70°C for 10 min.

3.2.5 Real-time quantitative PCR (qPCR)

The transcriptional regulation of selected genes was analyzed using real-time quantitative PCR (IQ^{TM} 5 Multicolor Real-time PCR detection system, BIO-RAD). Real-time PCR is a method based on the detection and quantification of a fluorescent reporter signal that increases in direct proportion to the amount of the PCR product in reaction (Livak *et al.*, 1995), (Lee *et al.*, 1993), using ABsolute^{TM} QPCR SYBR Green Mix (Thermo Fisher Scientific Inc, UK). CDNA was detected and quantified with the fluorescent dye SYBR Green, which offered a linear dose response over a wide range of target concentrations. As cDNA accumulates, the dye generates a signal that is proportional to the cDNA concentration. Fluorescein Dye acts as a passive reference dye to facilitate normalization of data. PCR reactions were performed in 25 µl volume by using the qPCR mix.

qPCR mix	Stock solution	Quantities per reaction
ABsolute™ QPCR SYBR Green fluorescein Mix	2x (Thermo-Start™ DNA Polymerase, Proprietary reaction buffer, dNTPs including dTTP, SYBR Green dye I, 3 mM MgCl2, Fluorescein Dye)	12.5 µl
Forward primer	10 pmol/µl	0.25 µl
Reverse primer	10 pmol/µl	0.25 µl
H2O		11 µl
cDNA derived from 1µg RNA		1 µl

Cycling conditions were as follows:

cycle 1: 95°C for 15 min;

cycle 2: 44 cycles of 95°C for 15 s, 55°C for 15 s and 72° C for 30 s;

cycle 3: 95°C for 30 s, 60°C for 30 s;

cycle 4: 71 cycles of 60°C for 10 s .

Formation of a single specific PCR product was confirmed by melting curve analysis. β-actin served as a reference gene for all real-time PCR reactions. Relative changes in gene expression were determined with the ΔCt method using the following formula: ΔCt = (Ct reference – Ct target). (Livak and Schmittgen, 2001).

3.2.6 Immunocytochemistry analysis

The immunocytochemistry analysis was measured by Catalyzed Signal Amplification (CSA) System (Dako, Hamburg, Germany).

On the first day, T24, UMUC-3 and EJ-28 cells were plated on 8-well glass chamber slides (Nalge Nunc International, Naperville, IL) at 6000/cm^2, 12000/cm^2 and 5000/cm^2, respectively. On the second day the cells were transfected with si-Random

or si-MAGE-A3 according to the transfection protocol. The cells were cultured for 72 hours after transfection, and then the cells were measured by CSA system. The cells on slides were fixed in 4 % paraformaldehyde for 10 min, and then were washed in PBS. The slides were immersed in Target Retrieval Solution and were heated up to 90 ^{o}C for 20 min. The slides were washed in TBST for 5 min. The slides were then incubated sequentially with hydrogen peroxide, Protein Block reagent, Primary antibody (Anti-human MAGE-A3, 1:50 dilution) (for negative control, the negative control reagent was used instead), Link Antibody, Streptavidin-Biotin Complex, Amplification Reagent, then Streptavidin-Peroxidase Reagent, and each incubation was followed by one wash with TBST. Substrate-Chromogen Solution was applied to cover specimen for 5 min at RT and the slides were rinsed gently with distilled water. The slides were immersed in hematoxylin, and then were rinsed gently with distilled water. The slides were then washed sequentially by dipping ten times each in: 70% ethanol, 100% ethanol, Xylenes. Specimen was mounted by glass coverslips using mounting medium. Images were acquired as JPEG format files with a Axiovert 200 Inverted microscope (Carl Zeiss Light Microscopy, Göttingen, Germany).

3.2.7 Cell count assay

Cell proliferation was measured by cell count assay. This method is to count cells from distinct groups with different treatment. On the first day, T24, UMUC-3 and EJ-28 cells were plated on 60mm diameter dishes at 6000/cm^2, 12000/cm^2 and 5000/cm^2, respectively. Each cell line consisted of two dishes, as one dish for each si-RNA(si-Random, si-MAGE-A3). On the second day the cells were transfected with si-RNA according to the transfection protocol. The cells were cultured 72 hours after transfection. Then the cells from each respective dish were detached using trypsin and counted.

3.2.8 Colony formation assay of cells in vitro

Colony formation assay is an in vitro microbiology technique for studying the effectiveness of specific agents on the survival and proliferation of cells based on the ability of a single cell to grow into a colony. The colony is defined to consist of at least 50 cells. The assay essentially tests every cell in the population for its ability to undergo ‘‘unlimited’’ division.

For this assay three cell lines were characterized: T24, UMUC-3 and EJ-28. Two 60mm diameter dishes were seeded from each cell line, with one dish for each si-RNA (si-Random, si-MAGE-A3). On the second day, the cells were transfected according to the transfection method. On the third day, they were trypsinized with 1 x trypsin for approximate 5 min at 37°C. The reaction was stopped by adding medium with 10% FCS containing trypsin inhibitors. For continuous culture three 60mm diameter dishes were established from each dish of these three cell lines at appropriate densities (T24 500cells/dish, UMUC-3 400cells/dish, EJ-28 300cells/dish). And then the cells were incubated for 14 days. After that , medium of the dishes was discarded and dishes were washed with 1x PBS, and then 2 ml of crystal violet stain (0.1% crystal violet, 10% formaldehyde, PBS) was added to each dish and incubated for 15 min at RT. The crystal violet stain was discarded and dishes were washed by tap water. The dishes were left to dry in normal air at room temperature. Then the colonies were counted.

3.2.9 2,3-Bis(2-methoxy-4-nitro-5-sulfophenyl)-2H-tetrazolium-5-carbox-anilide (XTT) viability assay

Cell viability was assessed by TACS® XTT kit (Trevigen Inc., Gaithersburg, USA). The use of tetrazolium salts, including XTT (2,3-Bis(2-methoxy-4-nitro-5-sulfophenyl)-2H-tetrazolium-5-carbox -anilide), to assay cell proliferation, cell viability, and/or cytotoxicity is a wide-spread, established practice. Cleavage of the tetrazolium salt to formazan occurs via the succinate-tetrazolium reductase system in the mitochondria of metabolically active cells. XTT, a yellow tetrazolium salt, is

cleaved to a soluble orange formazan dye, which can be measured by absorbance at 490 (or 450) nm in a microplate reader. (* modified from the instruction of the kit)

For this assay three cell lines were characterized: T24, UMUC-3 and EJ-28. One day before experiment, cells were seeded in a 96-well plate at varying densities (T24 3300cells/well, UMUC-3 9000cells/well, EJ-28 3600cells/well) in 100 µl medium, with triplicate wells for each si-RNA (si-Random, si-MAGE-A3) of each cell line. On the second day, transfection of si-RNA was performed as described in transfection method. The plate was incubated for 72 h. On the fourth day, the plate was measured by XTT assay. To prepare XTT Working Solution, XTT reagent and activator were warmed to 37°C for several minutes. Immediately before use, 100 µl of the XTT activator was added to 5 ml of XTT reagent to make XTT Working Solution. 50µl of prepared XTT Working Solution was added to each well, and then the plate was incubated for 4 hours at 37°C under 5% CO2. The absorbance of samples at 490 nm was measured by spectrofluorometer (FL-600) (BioTek Instruments GmbH, Bad Friedrichshall, Germany).

3.2.10 Measurement of cell apoptosis

Cell apoptosis was measured by TumorTACS™ In Situ Apoptosis Detection kit (Trevigen, Gaithersburg, USA)**.** This Kit is designed specifically for the detection of DNA fragmentation in cancer cells in culture.

A common biochemical marker of apoptosis is DNA fragmentation. During apoptosis the chromosomal DNA is cleaved by endonucleases to generate DNA fragments with free 3'-hydroxyl residues. In situ, the 3' ends of cleaved DNA fragments provide a substrate for the enzyme terminal deoxynucleotidyl transferase (TdT) which adds nucleotides at the site of DNA breaks. The incorporation of biotinylated nucleotides allows chromosomal DNA fragmentation to be visualized by binding streptavidin-horseradish peroxidase followed by reaction with diaminobenzidine (DAB) to generate a dark brown precipitate (* modified from the instruction of the

kit).

For this assay T24 cells were employed. On the first day, cells were seeded at 6000 cells/cm^2 in 400 µl of medium on an 8-well chamber slide. On the second day, transfection of si-RNA was performed as described in transfection method. The slide was incubated for 72 h. On the fifth day, the slide was measured by the apoptosis assay. The medium was removed and cells were rinsed once with 1X PBS at room temperature. The cells were incubated for 10 minutes at room temperature in 3.7% buffered formaldehyde. The slide was washed once in 1X PBS. After that, the samples were immersed in 1X PBS for 10 minutes and then were covered with 50 µl Cytonin^{TM} for 30 minutes. The slide was washed two times in deionized water. The samples were immersed in Quenching Solution for 5 minutes and then were washed in 1X PBS for 1 minute. Afterwards, the samples were immersed in 1X TdT Labeling Buffer for 5 minutes and then were incubated with 50 µl of Labeling Reaction Mix for 60 minutes at 37 ˚C in a humidity chamber. The samples were then immersed in 1X TdT Stop Buffer for 5 minutes followed with one wash in 1X PBS. Then the samples were incubated with 50 µl of Strep-HRP Solution for 10 minutes at room temperature in a humidity chamber to avoid evaporation. The slide was washed two times in 1X PBS and then was immersed in DAB solution for 2 to 7 minutes. After that, the slide was washed 4 times in deionized H2O and was subsequently immersed in 1% Methyl Green for 30 seconds. The slide was dipped sequentially in deionized water, 95% ethanol, 100% ethanol, then xylene. Samples were mounted by glass coverslips using mounting medium. Images were acquired as JPEG format files with the Axiovert 200 Inverted microscope. Cells containing fragmented nuclear chromatin characteristic of apoptosis will exhibit a brown nuclear staining that may be very dark after labeling, whereas cells without brown staining were defined as non-apoptotic cells.

3.2.11 Expression analysis of the relative levels of cell cycle and apoptosis related proteins

Analyzing the expression profiles of cell cycle and apoptosis related proteins is

helpful for understanding the roles these signaling molecules play in mechanisms related to programmed cell death and cell cycle. This assay was measured by Proteome Profiler^{TM} Array Human Apoptosis Array Kit (R&D systems, Inc., Minneapolis, USA). The Human Apoptosis Array is a rapid and sensitive tool to simultaneously detect the relative levels of expression of 35 cell cycle and apoptotic proteins.

For this assay T24 cells were employed. On the first day, cells were plated on 10cm diameter dishes at 6000 cells/cm^2. On the second day, transfection of si-RNA was performed as described in transfection method. The dishes were incubated for 72 h. On the fifth day, the dishes were rinsed with PBS and were added with lysis buffer. The cells were resuspended by pipetting up and down and then were rocked gently at 2-8 °C for 30 minutes. The cell lysates were centrifuged at 14,000 x g for 5 minutes, and then the supernatants were transfered into clean test tubes.

Quantitation of sample protein concentrations was performed with Pierce BCA protein assay (Pierce, Rockford, USA). In this assay, a series of dilutions of known concentration of bovine serum albumin (BSA) and protein samples with 1:10 dilution by dest. H_2O were prepared. Working solution was prepared by mixing 50 parts of BCA reagent A with 1 part of BCA reagent B (reagent A:B, 50:1). Then 200 µl working solution was added to each well after pipetting 25 µl of each standard or unknown sample replicate into a 96 well plate. After incubation of the plate at 37°C for 30 min, the absorbance of samples at 492 nm was measured by spectrofluorometer (FL-600) (BioTek Instruments GmbH, Bad Friedrichshall, Germany) and concentration of protein was determined based on the standard curve.

We used 400 µg of each sample for the next steps. 2 ml of blocking buffer was pipetted into each well of a 4-well multi-dish. One array was placed into each well of the 4-well multi-dish and was incubated for 1 hour on a rocking platform shaker. While arrays were blocking, the samples were prepared by adding the desired quantity of lysate to 1.25 ml of the blocking buffer and then were adjusted to a final volume of

1.5 ml with Lysis Buffer as necessary. The buffer was removed from the multi-dish. Prepared samples were added into the multi-dish and the dish was incubated overnight at 2-8 °C on a rocking platform shaker. Each array was placed into individual plastic containers containing 20 ml of Wash Buffer. The arrays were washed with Wash Buffer for 10 minutes on a rocking platform shaker and this step was repeated two times for a total of three washes. For each array, 15 µl of reconstituted Detection Antibody Cocktail was diluted to 1.5 ml with Array Buffer. 1.5 ml of diluted Detection Antibody Cocktail was pipetted into each well of the multi-dish. Each array was returned to the multi-dish containing the diluted Detection Antibody Cocktail. The arrays were incubated for 1 hour on a rocking platform shaker. Each array was washed as described previously. The Streptavidin-HRP was diluted in Array Buffer and 2 ml of diluted Streptavidin-HRP was pipetted into each well of the 4-well multi-dish. Each membrane was returned to the 4-well multi-dish containing the diluted Streptavidin-HRP. After that, the arrays were incubated for 30 minutes on a rocking platform shaker and then were washed as described previously. Each membrane was placed on the bottom sheet of a plastic sheet protector with the identification number facing up. The arrays were detected by ECL (Enhanced Chemi-luminescence, Amersham, Germany) treatment, followed by exposure of the membrane in FluorChem^{TM} 8900 chemi-luminescence imager (Alpha Innotech, California, USA). Quantitation of signal intensity was performed with the AlphaEase FC software (Alpha Innotech, California, USA).

3.3 Statistical analysis

All the data in the figures and text are expressed as means ± SEM of n independent observations unless indicated otherwise. Statistical evaluation was performed by paired t-test.

4. Results

4.1 Expression studies of MAGE-A3 in a panel of different bladder cancer cell lines.

At first, we analyzed the expression of MAGE-A3 in different bladder cancer cell lines. MAGE-A3 mRNA was analyzed by quantitative realtime RT-PCR in T24, HT-1376, BFTC-905, 5637, EJ-28, and UMUC-3 cells (Figure 3A). High levels of MAGE-A3 mRNA were observed in T24, UMUC-3 and 5637 cells, whereas no detectable levels were observed in EJ-28 cells. BFTC-905 and HT-1376 cells exhibited intermediate MAGE-A3 mRNA levels. Transfection of cells with a control siRNA(si-Random) had no effect on MAGE-A3-mRNA levels when compared to non-treated cells (Figure 3B).

A

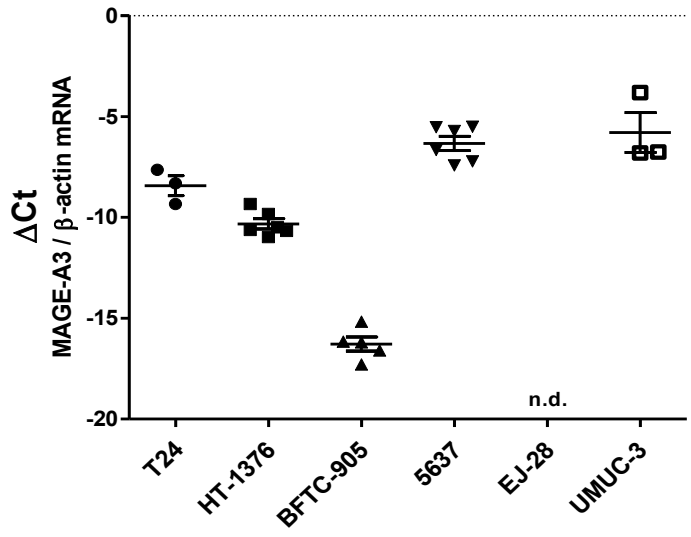

B

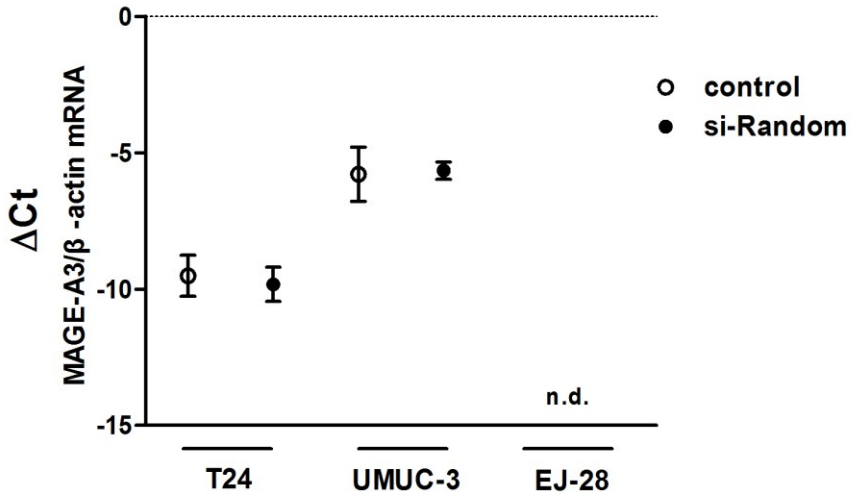

Figure 3: The expression of MAGE-A3 in different bladder cancer cell lines

A: Quantification of MAGE-A3 mRNA levels by real time RT-PCR of RNA extracts from T24, HT-1376, BFTC-905, 5637, EJ-28, and UMUC-3 cells. Different batches of cultured cells available in our laboratory were measured. The respective n-number is reflected by the number of symbols indicated $3 \leq n \leq 6$) . β-actin mRNA was used as reference for ΔCt calculation. The highest MAGE-A3-mRNA concentrations are observed in UMUC-3 cells followed by T24 cells. In EJ-28 cells, MAGE-A3-mRNA was not detectable. Values are presented as mean, SEM, as well as single values (n.d., non-detectable). **B:** MAGE-A3 mRNA analysis of RNA extracts from T24, UMUC-3 and EJ-28 cell lines. MAGE-A3-mRNA levels of naïve cells (control) were compared to cells that were transfected with control siRNA (si-Random). Values are presented as mean, SEM, n=3. No significant differences were obvious (paired t-test: $p>0.05$).

4.2 Establishment of selective silencing of MAGE-A3 by RNA interference (siRNA)

For analyzing the biological function of MAGE-A3, knockdown (silencing) of MAGE-A3 expression by RNA interference was established. We transfected small interfering RNA (si-RNA) targeting MAGE-A3 (si-MAGE-A3) compared to a non-target control si-RNA (si-Random). The silencing effect was validated by real time RT-PCR analysis of mRNA extracts from the transfected cells. An approximate down-regulation of MAGE-A3 mRNA level by 80 % was observed in T24 and UMUC-3 cells transfected with si-MAGE-A3 when compared to si-Random treated cells, whereas no detectable MAGE-A3 levels were observed in non-MAGE-A3 expressing EJ-28 cells (Figure 4A). Moreover, silencing of MAGE-A3 expression was supported at the protein level by immunocytochemistry analysis showing weaker cytoplasmic staining in T24 and UMUC-3 cells treated with si-MAGE-A3 when compared to si-Random treated cells. No obvious difference in staining could be observed between si-MAGE-A3 and si-Random groups in EJ-28 cells (Figure 4B).

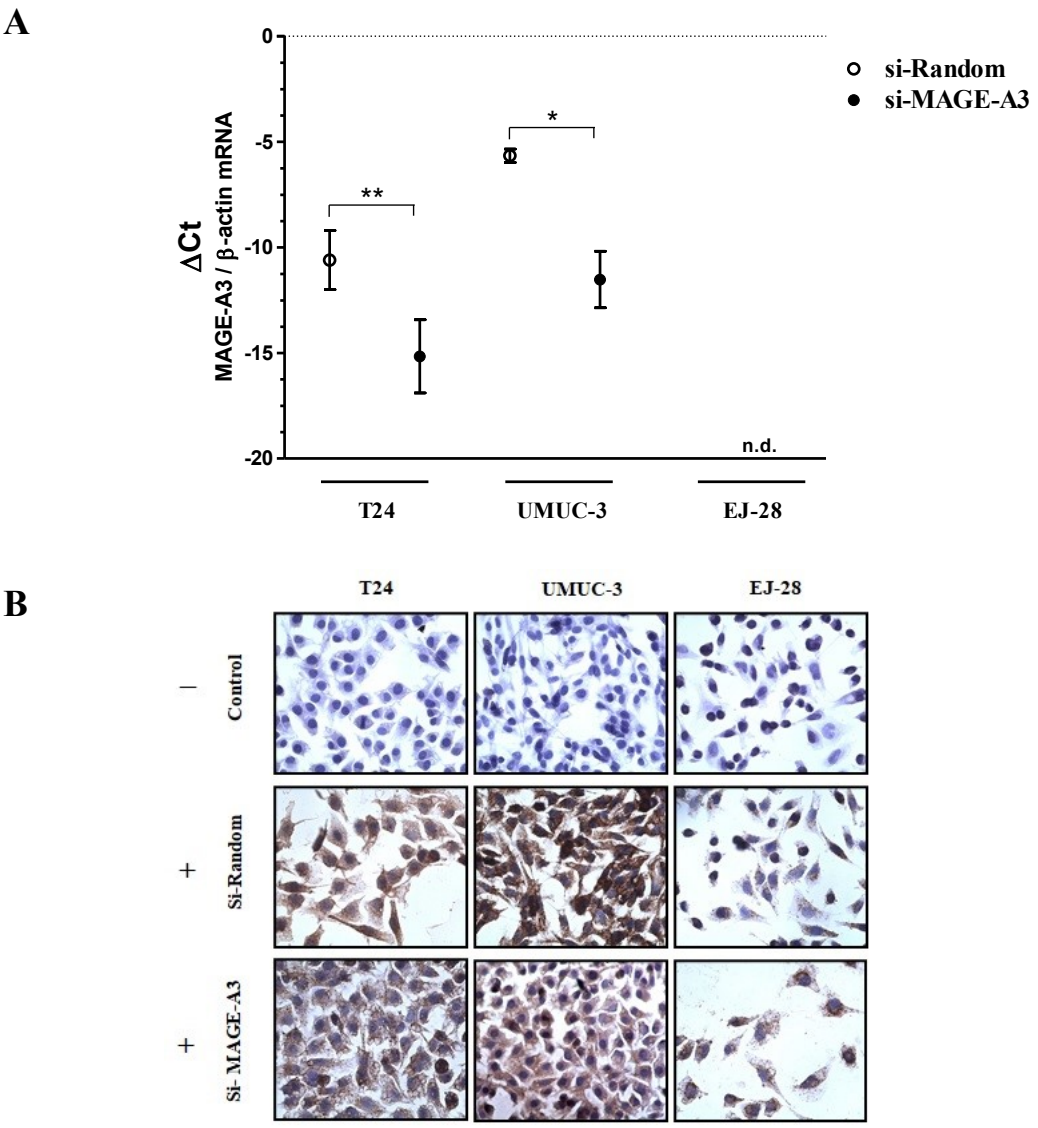

Figure 4: Silencing of MAGE-A3 expression by si-RNA

A: MAGE-A3 mRNA analysis by real time RT-PCR of RNA extracts from T24, UMUC-3 and EJ-28 cells transfected with si-MAGE-A3 or si-Random (n.d.: non-detectable). Values are presented as mean, SEM, n=3. Significant differences, paired t-test: *$p<0.05$, **$p<0.01$. **B:** Immunocytochemistry of MAGE-A3. In the upper lane, non-treated control cells (control) without primary anti-MAGE-A3 antibody are displayed (-). In the lower two lanes, cells are shown that were transfected with si-Random or si-MAGE-A3. Here, the MAGE-A3 antibody was included (+). In the Si-Random lane, obvious immunostaining was observed in T24 and UMUC-3 cells (brown color) when compared to control group (without MAGE-A3-antibody). In si-MAGE-A3 treated T24 and UMUC-3 cells, the staining appears weaker. In comparison, immunostaining of EJ-28 cells without detectable MAGE-A3-mRNA appears less intensive (close to background level).

4.3 Effects of silencing of MAGE-A3 on cell proliferation and viability

In order to analyze whether MAGE-A3 affects oncogenicity in bladder cancer cells, we performed assays regarding cell proliferation and viability after silencing of MAGE-A3. To follow this aim we employed the following three different methods.

The first method used was cell count analysis. As shown in Figure 5, the cell numbers of T24 and UMUC-3 cell lines were both significantly increased when transfected with si-MAGE-A3 as compared to si-Random treated cells, whereas there was no significant difference between si-MAGE-A3 and si-Random groups in EJ-28 cells.

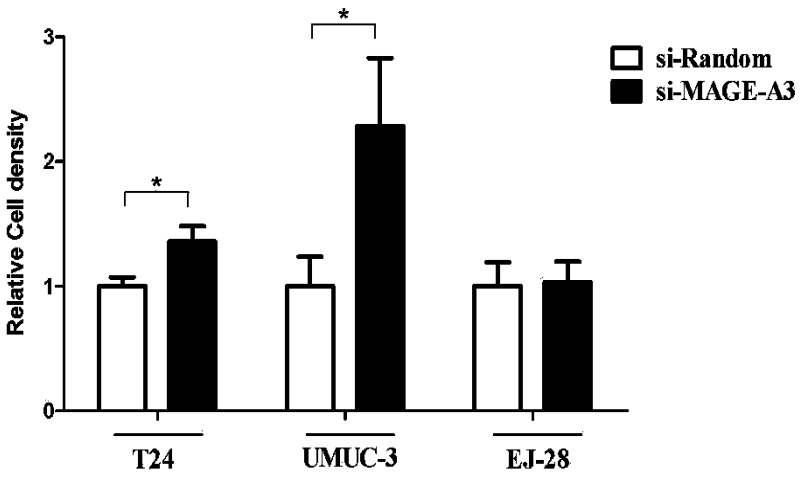

Figure 5: Effect of silencing MAGE-A3 on cell proliferation by cell count assay
Presented are the relative cell densities of si-Random group (normalized to 1) and the si-MAGE-A3 group. Values are presented as mean, SEM, n=3. Significant differences, paired t-test: *$p<0.05$.

The second method used was colony formation assay. As shown in Figure 6, suppression of MAGE-A3 by si-MAGE-A3 resulted in significant increases of colony number in T24 and UMUC-3 cells as compared to si-Random, whereas no significant difference was observed in EJ-28 cells.

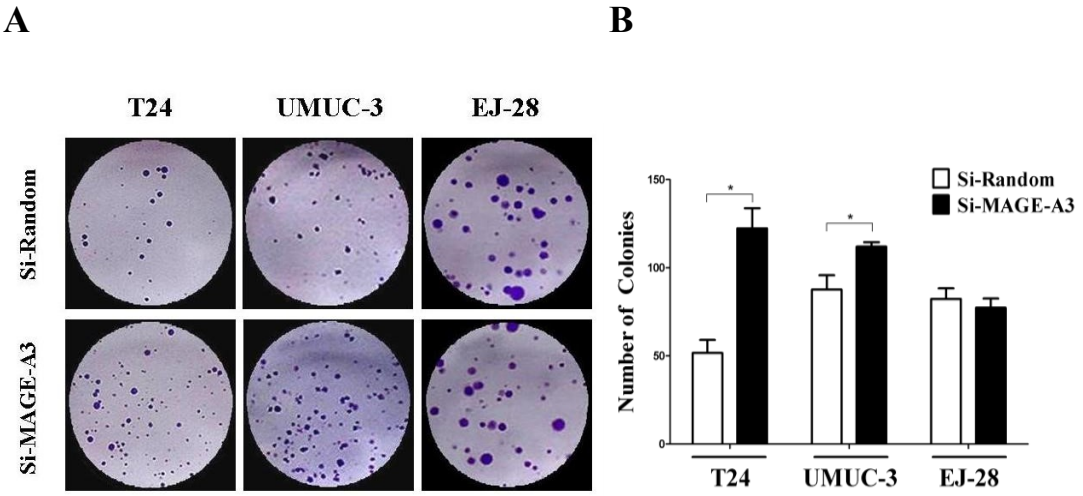

Figure 6: Effect of silencing MAGE-A3 on cell viability by colony formation assay
A: Colony formation assay showing that silencing of MAGE-A3 resulted in significantly increased outgrowth of T24 and UMUC-3 cells, whereas there was no significant difference in EJ-28 cells. **B:** Quantitative analysis: a colony was defined to consist of at least 50 cells. The colony numbers were measured from T24, UMUC-3 and EJ-28 cells transfected with si-MAGE-A3 or si-Random. Values are presented as mean, SEM, n=3. Significant differences, paired t-test: *$p<0.05$).

The third method used was XTT assay, a viability assay which strongly correlates with cell proliferation. In accordance with the previous observations, this assay showed significant increases of viable cells in T24 and UMUC-3 cells transfected with si-MAGE-A3 when compared to si-Random, while no significant difference was observed in EJ-28 cells (Figure 7).

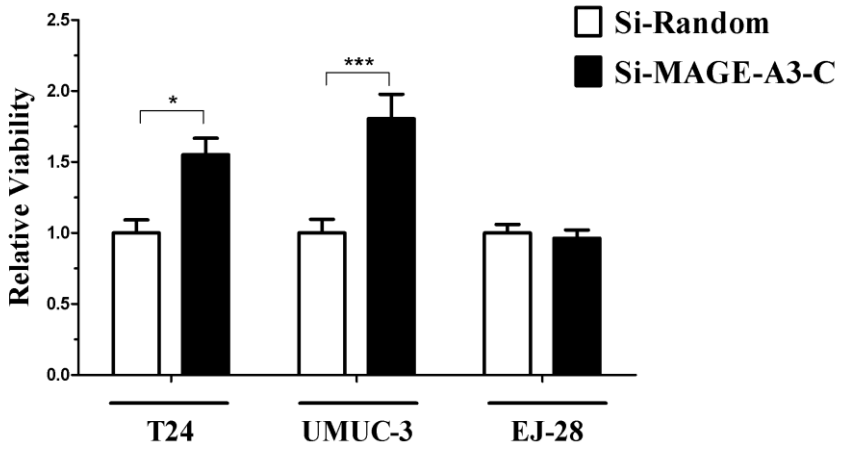

Figure 7: Effect of silencing MAGE-A3 on cell proliferation (XTT assay)
The relative values (si-Random group normalized to 1) are shown. Values are presented as mean, SEM, significant differences between si-MAGE-A3 and si-Random groups, n=6 (T24), n=9 (UMUC-3 and EJ-28), paired t-test: *p<0.05, ***p<0.001.

4.4 Effect of silencing of MAGE-A3 on cell apoptosis

Next, we analyzed potential effect of MAGE-A3 on apoptosis by Tunel assay based on DNA laddering in T24 cells.

As depicted in Figure 8, this assay showed a decreased occurence of apoptosis in the si-MAGE-A3 group when compared with si-Random group. Since the incidence of apoptosis was observed at a low level below 1%, the biological significance of this finding remains unclear.

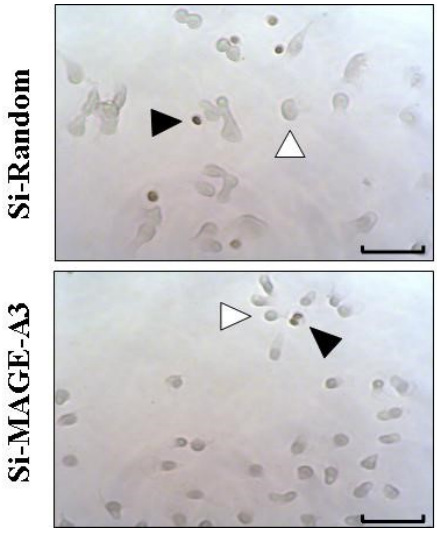

Table 2 : Quantitative analysis of the Tunel assay

Group	Number of apoptotic cells	Total Number of cells	Incidence of apoptosis
Si-random	245	24700	1%
Si-MAGE-A3	122	38300	0.3%

Figure 8: Apoptosis analysis after silencing of MAGE-A3 in T24 cells
Microscopic analysis of cell apoptosis by in situ Tunel assay after silencing MAGE-A3 in T24 cells (▲ indicates apoptotic cells, △ indicates non-apoptotic cells. Bar scale represents 50μm).
Table 2 : Quantitative analysis of the Tunel assay.
Silencing of MAGE-A3 resulted in decreased apoptotic incidence when compared to si-Random group.

4.5 Expression analysis of the relative levels of cell cycle and apoptosis related proteins

In order to analyze possible signal transduction pathways that are responsible for changes in cell proliferation and viability, we performed proteomic array analysis of T24 cells treated with si-MAGE-A3 compared to si-Random. We observed most striking differences in up-regulation of livin and down-regulation of cyclin-dependent kinase inhibitor p21 and differently phosphorylated p53 (tumor suppressor) forms. These changes may contribute to the enhanced survival and proliferation observed in the si-MAGE-A3 treated group (Figure 9).

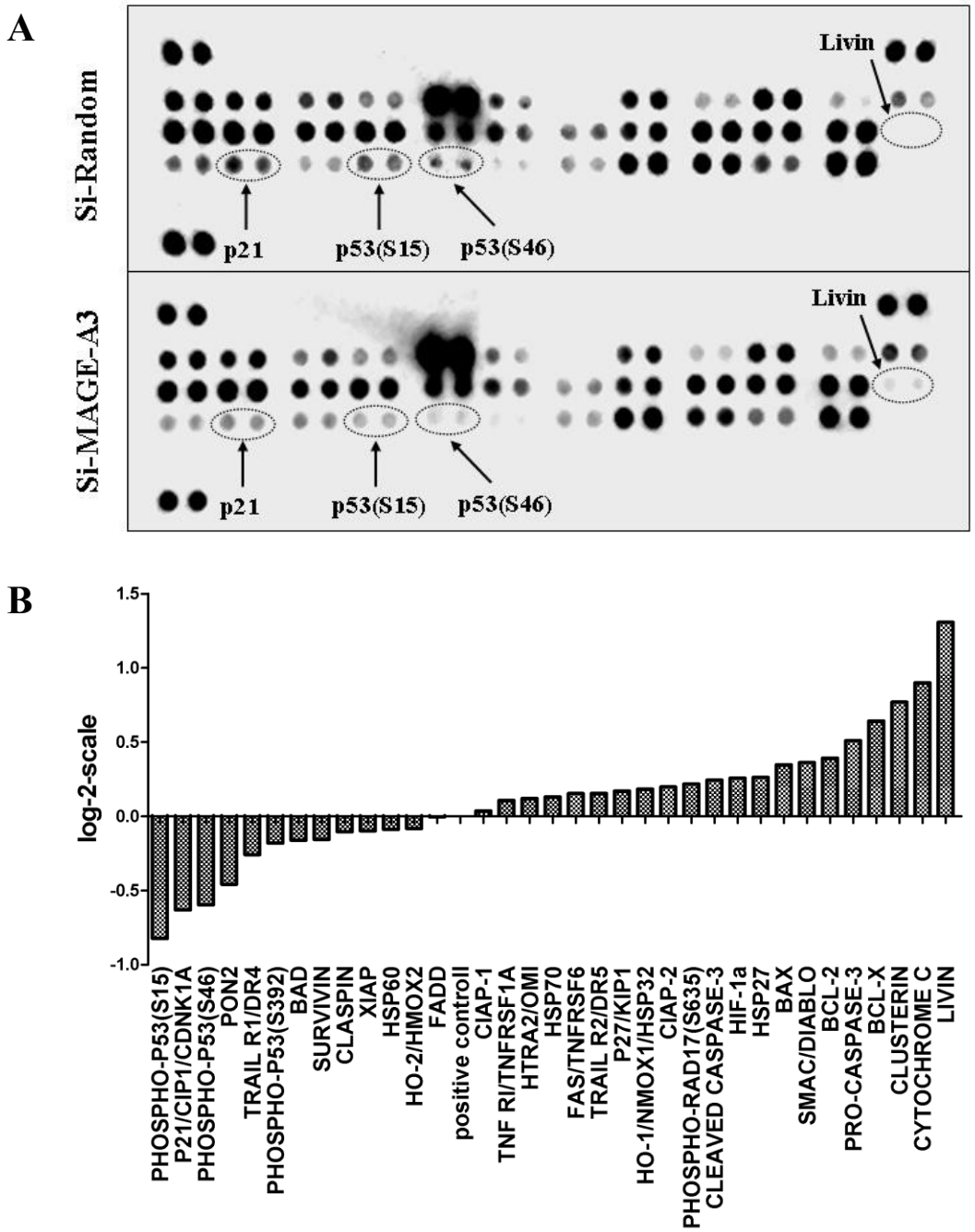

Figure 9: Expression analysis of the relative levels of cell cycle and apoptosis related proteins

A: Autoradiography of proteomic array of cell cycle and apoptotic proteins in T24 cells treated with si-Random or si-MAGE-A3. **B:** Quantitative analysis by densitometric scanning and normalization of protein signals from the autoradiography. Displayed is the fold-change of signal intensity in si-MAGE-A3 compared to si-Random treated group. All names of protein from the array are named.

5. Discussion

So far, the expression of MAGE-A3 has mainly been studied in bladder cancer tissues (Dyrskjot *et al.*, 2012; Sharma *et al.*, 2006; Yin *et al.*, 2011) whereas possible functions of MAGE-A3 in bladder cancer cell lines are largely unknown. Functional analyses about MAGE were performed in melanoma cells, myeloma cells, lung cancer cells, breast cancer cells, ovarian cancer cells, and others (Atanackovic *et al.*, 2010; Duan *et al.*, 2003; Monte *et al.*, 2006; Nardiello *et al.*, 2011; Peikert *et al.*, 2006; Xia *et al.*, 2012; Yang *et al.*, 2007). Against the background of these studies, we analyzed the expression and function of MAGE-A3 in a panel of human bladder cancer cell lines.

According to our analysis of MAGE-A3 expression, we could demonstrate quite different expression patterns of MAGE-A3 mRNA in human bladder cancer cell lines including cells with relative high (T24, 5637 and UMUC-3 cells), intermediate (HT-1376, BFTC-905 cells) and nondetectable levels (EJ-28 cells). We selected two cell lines with high MAGE-A3 mRNA expression (T24, UMUC3) and one cell line with nondetectable MAGE-A3 mRNA expression (EJ-28) serving as control cells for the functional studies.

It has to be mentioned that the selection of cells was mainly based on quantitative mRNA expression analysis of cell lines since subtype specific analysis of MAGE-A3 at the protein level is difficult to perform due to the high conservation between MAGE-A family members (Figure 10). Thus, it is difficult to develop antibodies that can distinguish different MAGE proteins. Anti-MAGE antibodies may cross-react with other MAGE subtypes. For instance, the anti-MAGE-A3 antibody employed cross-reacts with MAGE-A1, -A4, -A6, and -A12 (Busam *et al.*, 2000; Rimoldi *et al.*, 2000). Detection of MAGE-A3 at the mRNA level has the advantage to allow improved differentiation between different MAGE subtypes. Thus, studying MAGE-A3 expression at the protein level by immunocytochemistry may reflect the

sum of signals derived from different MAGE subtypes.

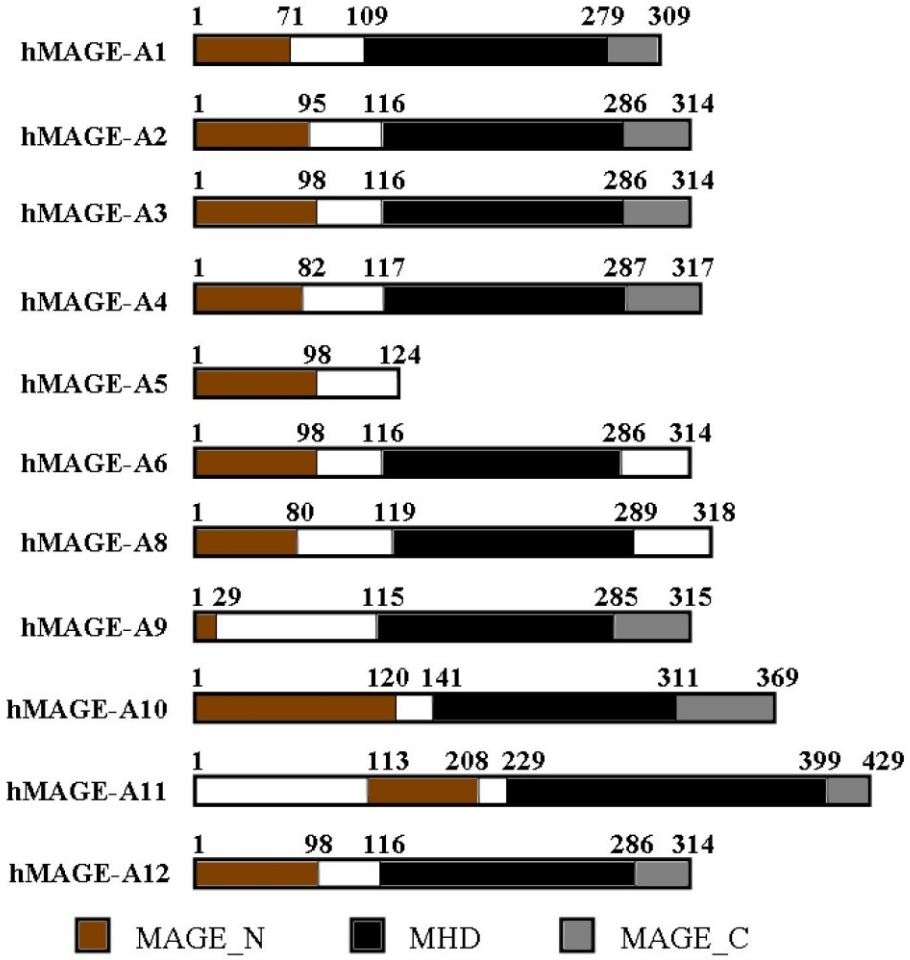

Figure 10: Structural feature of the human MAGE-A family proteins (MAGEA1, -A2, -A3, -A4, -A5, -A6, -A8, -A9, -A10, -A11, -A12) except for MAGE-A7 (pseudogenes)
MAGE NH_2-terminal region (MAGE_N), MAGE homology domain (MHD) and MAGE COOH-terminal region (MAGE_C) are indicated. There are no predicted domains in MAGE_N and MAGE_C regions.
*Figure modified from Sang M et al.(Sang *et al.*, 2011a).

We established an effective way for silencing of MAGE-A3 by siRNA for investigating the biological function of MAGE-A3 in bladder cancer cells. Based on in silico screening, we could identify one siRNA motif that potently inhibited the expression of MAGE-A3 in T24 and UMUC-3 cells. Employing this siRNA sequence we performed the functional experiments.

These experiments included analyses of cell proliferation, colony formation and

apoptosis. We observed inhibition of cell proliferation and survival mediated by MAGE-A3 whereas apoptosis was increased.

For identifying possible signal transduction pathways affected by MAGE-A3, proteomic array analysis of proteins regulating cell cycle and apoptosis was performed. We found most striking differences in up-regulation of livin and down-regulation of p21 and differently phosphorylated p53 forms after silencing of MAGE-A3.

Interestingly, our results suggested that MAGE-A3 might play an important role in inhibition of survival of bladder cancer cells and it might have an anti-oncogenic function. In contrast, MAGE-A3 subtype has been mainly attributed to exert pro-proliferative and anti-apoptotic characteristics. Djordje Atanackovic et al. (Atanackovic *et al.*, 2010) demonstrated that MAGE-A3 promoted the survival of multiple myeloma cells by suppressing apoptosis. It was reported that down-regulation of type I MAGE proteins including MAGE-A3 led to p53 transcriptional induction and p53-dependent apoptosis in melanoma and myeloma cells (Nardiello *et al.*, 2011; Yang *et al.*, 2007). It was also shown that inhibition of MAGE-A3, which resulted in p53 and p21 accumulation, could reduce the proliferation of pituitary cells (Zhu *et al.*, 2008). These studies displayed effects of MAGE-A3 on cell survival and apoptosis. In our study, we identified livin, p21 and phosphorylated p53 forms as important targets that were markedly altered by MAGE-A3 as revealed by proteomic array approach and it demonstrated increased level of livin and decreased levels of p21 and phospho-p53 forms after silencing of MAGE-A3. Livin is considered as a member of the inhibitors of apoptosis family, and it promotes cell growth and inhibits apoptosis (Wang *et al.*, 2010; Yang *et al.*, 2010). p21 is a cyclin-dependent kinase inhibitor encoded by the CDKN1A gene in humans and functions as a regulator of cell cycle progression at G_1 (el-Deiry *et al.*, 1993; Harper *et al.*, 1993; Li *et al.*, 2011). p53 is a tumor suppressor protein encoded by the TP53 gene in humans and functions as a tumor suppressor that is related to preventing

cancer (Brosh and Rotter, 2010; Kern *et al.*, 1991; Matlashewski *et al.*, 1984; Paolella *et al.*, 2011). Therefore, MAGE-A3 may inhibit survival and induce apoptosis of bladder cancer cells through inhibiting the expression of livin and augmenting the expression of p21 and phospho-p53 forms.

Thus, our results suggest that MAGE-A3 does not only represent a tumor antigen but may inhibit cell survival and induce apoptosis. Surprisingly, these functions observed in bladder cancer cells are anti-oncogenic. They should be confirmed by further studies employing additional siRNA motifs. In our group, we tested several of them, however only one of them was functional operative. Furthermore, it is still unclear how livin, p21 and p53 are affected by MAGE-A3 at the molecular level. Direct or secondary interactions may be involved in this regard.

One further important aspect to clarify remains the question why MAGE-A3 has opposite functions in different cancer cell lines. So far, the relevant mechanisms are not clear. Differences in cell type specific components that interact with MAGE-A3 and that affect cell proliferation and apoptosis in a different way may be responsible. So far, only MAGE-A4 subtype has been linked to anti-oncogenic function as revealed by its pro-apoptotic characteristic in lung cancer cells. In this study, pro-apoptotic effects of MAGE-A4 could be attributed to enhanced caspase 3 cleavage (Peikert *et al.*, 2006). The functional accordance of MAGE-A4 in lung cancer cells and MAGE-A3 in bladder cancer cell lines may be related to the strong structural homology between MAGE-A3 and MAGE-A4 (Figure 10).

At present, clinic trials of MAGE-A3 vaccination protocols are tested in bladder cancer. This treatment may initiate a cytotoxic immunresponse against tumor cells bearing MAGE-A3 antigens. In this approach, MAGE-A3 is targeted as a tumor selective antigen without considering any functional aspects of MAGE-A3. Based on our findings that MAGE-A3 may exert some anti-oncogenic function regarding proliferation and apoptosis, it would be of interest to analyse that to which extent

immunologic therapy targeting MAGE-A3 might affect anti-oncogenic function in bladder cancer cells.

6. Summary

6.1 Summary

MAGE-A3 is a member of the type I Melanoma Antigen Gene family and is expressed in various cancers including bladder cancer. MAGE-A3 represents a candidate antigen as a possible target for cancer immunotherapy. In particular, MAGE-A3 vaccination protocols are investigated in clinical trials in bladder cancer. So far, functional studies on MAGE were mainly performed in melanoma cells, myeloma cells, lung cancer and breast cancer cells whereas the function of MAGE-A3 in bladder cancer cells is largely unknown.

Here, we analyzed the expression of MAGE-A3 in a panel of human bladder cancer cell lines and selected appropriate cells for functional studies. Furthermore, we established potent knockdown of MAGE-A3 by RNA interference and harnessed this technique for functional analysis of MAGE-A3. MAGE-A3 mRNA levels where highest in UMUC-3, 5637 and T24 cells whereas no detectable levels were observed in EJ-28 cells. BFTC-905 and HT-1376 cells exhibited intermediate MAGE-A3 mRNA levels. For further experiments, T24, UMUC-3 and EJ-28 cells were selected and MAGE-A3 expression was confirmed at protein level by immunocytochemistry. Potent siRNA knockdown of MAGE-A3 mRNA was validated by RT-PCR exhibiting down-regulation of MAGE-A3 mRNA by approximately 80 % in T24 and UMUC-3 cells. Evidence of MAGE-A3 knockdown could also be confirmed in a non-quantitative way by immunocytochemistry. EJ-28 cells that displayed no detectable MAGE-A3 mRNA abundance were included in these experiments as control cells.

At the functional level, silencing of MAGE-A3 resulted in significant increased proliferation, cell count and colony formation in T24 und UMUC-3 cells, whereas EJ-28 cells were unaffected. Apoptosis was reduced after silencing of MAGE-A3 in

T24 cells. In order to get some mechanistic clue for this observation, proteomic array analysis of cell cycle regulatory and apoptotic proteins was performed in T24 cells demonstrating increased level of livin and decreased levels of cyclin-dependent kinase inhibitor p21 and tumor suppressor protein phospho-p53 forms after silencing of MAGE-A3. Thus, at the functional level we could demonstrate anti-proliferative and pro-apoptotic effects of MAGE-A3 indicating an anti-oncogenic characteristic. The anti-proliferative and pro-apoptotic effects of MAGE-A3 were accompanied by down-regulation of livin and up-regulation of p21 and phospho-p53 forms likely contributing to or mediating the observed effects.

In sum, we selected suitable bladder cancer cell lines for analysis of MAGE-A3 and established efficient silencing of MAGE-A3. Interestingly, we revealed an important so far non-described anti-oncogenic function of MAGE-A3 in bladder cancer cells. This aspect should be considered when employing immunotherapeutic strategies targeting MAGE-A3 tumor antigen by antibodies.

6.2 Zusammenfassung

MAGE-A3 ist ein Mitglied der Typ I Melanom Antigen Familie und kommt in verschiedenen Krebsarten, darunter auch Blasenkrebs, vor. MAGE-A3 repräsentiert ein mögliches Antigen für eine gezielte Krebs-Immunotherapie. So werden momentan MAGE-A3 Impfprotokolle für Blasenkrebs in klinischen Studien untersucht. Bisher erfolgten funktionelle Studien zu MAGE in Melanom-, Myelom-, Lungenkrebs- und Brustkrebszellen, während die Funktion von MAGE-A3 in Blasenkrebszellen unklar ist.

In dieser Arbeit haben wir die Expression von MAGE-A3 in mehreren humanen Blasenkrebs-Zelllinien analysiert und geeignete Zellen für weitergehende Studien selektiert. Des Weiteren konnten wir eine stabile Suppression von MAGE-A3 durch RNA-Interferenz etablieren und diese Technik zur Funktionsanalyse von MAGE-A3 ausnutzen. MAGE-A3 mRNA Konzentrationen waren am höchsten in UMUC-3, 5637 und T24-Zellen, während in EJ-28 Zellen keine mRNA für MAGE-A3 detektierbar war. BFTC-905 und HT-1376 Zellen wiesen intermediäre MAGE-A3 mRNA-Konzentrationen auf. In weiteren Experimenten wurde die MAGE-A3 Expression an T24, UMUC-3 und EJ-28 Zellen auf Proteinebene mittels Immunzytochemie überprüft. Dabei zeigte sich deutliche MAGE-A3 Immunreaktivität an T24 und UMUC Zellen, die an EJ-28 Zellen weniger ausgeprägt auf Hintergrundsniveau erschien. Effektive Suppression von MAGE-A3 mRNA durch RNA-Interferenz wurde durch quantitative RT-PCR validiert, welche eine Inhibition um ca. 80% zeigte, die durch Immunzytochemie bestätigt wurde.

Auf funktioneller Ebene resultierte die Suppression von MAGE-A3 in signifikant erhöhter Proliferation, Zellzählung und Koloniebildung in T24 und UMUC-3 Zellen, während in EJ-28 Zellen keine Änderung zu beobachten war. T24 Zellen reagierten auf die Suppression von MAGE-A3 mit reduzierter Apoptose. Um diese Beobachtungen auf Signaltransduktionsebene fassen zu können, wurde an T24-Zellen

ein Proteom-Array von Zellzyklus und Apoptose regulierenden Komponenten durchgeführt. Hierbei zeigten sich bei den Zellen mit Suppression von MAGE-A3 verminderte Spiegel von Cyclin-abhängigem Kinaseinhibitor p21- und phosphorylierten p53- Tumorsuppressor Protein und ein erhöhter Spiegel von Livin, die das gesteigerte Überleben der Zellen erklären könnten.

Zusammenfassend haben wir geeignete Blasenkrebs-Zelllinien für die Analyse von MAGE-A3 identifiziert und an diesen Zellen eine effiziente Suppression von MAGE-A3 etabliert. Interessanterweise konnten wir eine bislang noch nicht beschriebene anti-onkogene Funktion von MAGE-A3 an diesen Zellen beobachten. Dieser Aspekt sollte bei der Entwicklung neuer Immunotherapieverfahren mit MAGE-A3 als Zielantigen berücksichtigt werde und entsprechende Effekte, die durch MAGE-A3 Antikörper ausgelöst werden, auf Tumorzellebene untersucht werden.

7. References

Amling CL (2001). Diagnosis and management of superficial bladder cancer. *Curr Probl Cancer* 25: 219-78.

Askew EB, Bai S, Blackwelder AJ, Wilson EM (2010). Transcriptional synergy between melanoma antigen gene protein-A11 (MAGE-11) and p300 in androgen receptor signaling. *J Biol Chem* 285: 21824-36.

Askew EB, Bai S, Hnat AT, Minges JT, Wilson EM (2009). Melanoma antigen gene protein-A11 (MAGE-11) F-box links the androgen receptor NH2-terminal transactivation domain to p160 coactivators. *J Biol Chem* 284: 34793-808.

Atanackovic D, Hildebrandt Y, Jadczak A, Cao Y, Luetkens T, Meyer S, Kobold S, Bartels K, Pabst C, Lajmi N, Gordic M, Stahl T, Zander AR, Bokemeyer C, Kroger N (2010). Cancer-testis antigens MAGE-C1/CT7 and MAGE-A3 promote the survival of multiple myeloma cells. *Haematologica* 95: 785-93.

Bai S, He B, Wilson EM (2005). Melanoma antigen gene protein MAGE-11 regulates androgen receptor function by modulating the interdomain interaction. *Mol Cell Biol* 25: 1238-57.

Bai S, Wilson EM (2008). Epidermal-growth-factor-dependent phosphorylation and ubiquitinylation of MAGE-11 regulates its interaction with the androgen receptor. *Mol Cell Biol* 28: 1947-63.

Bandic D, Juretic A, Sarcevic B, Separovic V, Kujundzic-Tiljak M, Hudolin T, Spagnoli GC, Covic D, Samija M (2006). Expression and possible prognostic role of MAGE-A4, NY-ESO-1, and HER-2 antigens in women with relapsing invasive ductal breast cancer: retrospective immunohistochemical study. *Croat Med J* 47: 32-41.

Barker PA, Salehi A (2002). The MAGE proteins: emerging roles in cell cycle progression, apoptosis, and neurogenetic disease. *J Neurosci Res* 67: 705-12.

Bergeron A, Picard V, LaRue H, Harel F, Hovington H, Lacombe L, Fradet Y (2009). High frequency of MAGE-A4 and MAGE-A9 expression in high-risk bladder cancer. *Int J Cancer* 125: 1365-71.

Brasseur F, Rimoldi D, Lienard D, Lethe B, Carrel S, Arienti F, Suter L, Vanwijck R, Bourlond A, Humblet Y, et al. (1995). Expression of MAGE genes in primary and metastatic cutaneous melanoma. *Int J Cancer* 63: 375-80.

Brosh R, Rotter V (2010). Transcriptional control of the proliferation cluster by the tumor suppressor p53. *Mol Biosyst* 6: 17-29.

Busam KJ, Iversen K, Berwick M, Spagnoli GC, Old LJ, Jungbluth AA (2000). Immunoreactivity with the anti-MAGE antibody 57B in malignant melanoma: frequency of expression and correlation with prognostic parameters. *Mod Pathol* 13: 459-65.

Chomez P, De Backer O, Bertrand M, De Plaen E, Boon T, Lucas S (2001). An overview of the MAGE gene family with the identification of all human members of the family. *Cancer Res* 61: 5544-51.

Chong CE, Lim KP, Gan CP, Marsh CA, Zain RB, Abraham MT, Prime SS, Teo SH, Silvio Gutkind J, Patel V, Cheong SC (2012). Over-expression of MAGED4B increases cell migration and growth in oral squamous cell carcinoma and is associated with poor disease outcome. *Cancer Lett* 321: 18-26.

Dabovic B, Zanaria E, Bardoni B, Lisa A, Bordignon C, Russo V, Matessi C, Traversari C, Camerino G (1995). A family of rapidly evolving genes from the sex reversal critical region in Xp21. *Mamm Genome* 6: 571-80.

De Plaen E, Arden K, Traversari C, Gaforio JJ, Szikora JP, De Smet C, Brasseur F, van der Bruggen P, Lethe B, Lurquin C, et al. (1994). Structure, chromosomal localization, and expression of 12 genes of the MAGE family. *Immunogenetics* 40: 360-9.

De Plaen E, De Backer O, Arnaud D, Bonjean B, Chomez P, Martelange V, Avner P, Baldacci P, Babinet C, Hwang SY, Knowles B, Boon T (1999). A new family of mouse genes homologous to the human MAGE genes. *Genomics* 55: 176-84.

Derré L, Cesson V, Lucca I, Cerantola Y, Valerio M, Fritschi U, Vlamopoulos Y, Burruni R, Legris AS, Dartiguenave F, Gharbi D, Martin V, Vaucher L, Speiser DE, Romero P, Jichlinski P, Nardelli-Haefliger D (2017). Intravesical Bacillus Calmette Guerin Combined with a Cancer Vaccine Increases Local T-Cell Responses in Non-muscle-Invasive Bladder Cancer Patients. *Clin Cancer Res* 23: 717–25.

De Smet C, Lurquin C, Lethe B, Martelange V, Boon T (1999). DNA methylation is the primary silencing mechanism for a set of germ line- and tumor-specific genes with a CpG-rich promoter. *Mol Cell Biol* 19: 7327-35.

Doyle JM, Gao J, Wang J, Yang M, Potts PR (2010). MAGE-RING protein complexes comprise a family of E3 ubiquitin ligases. *Mol Cell* 39: 963-74.

Duan Z, Duan Y, Lamendola DE, Yusuf RZ, Naeem R, Penson RT, Seiden MV (2003).

Overexpression of MAGE/GAGE genes in paclitaxel/doxorubicin-resistant human cancer cell lines. *Clin Cancer Res* 9: 2778-85.

Dyrskjot L, Zieger K, Kissow Lildal T, Reinert T, Gruselle O, Coche T, Borre M, Orntoft TF (2012). Expression of MAGE-A3, NY-ESO-1, LAGE-1 and PRAME in urothelial carcinoma. *Br J Cancer* 107: 116-22.

el-Deiry WS, Tokino T, Velculescu VE, Levy DB, Parsons R, Trent JM, Lin D, Mercer WE, Kinzler KW, Vogelstein B (1993). WAF1, a potential mediator of p53 tumor suppression. *Cell* 75: 817-25.

Espantman KC, O'Shea CC (2010). aMAGEing new players enter the RING to promote ubiquitylation. *Mol Cell* 39: 835-7.

Feng Y, Gao J, Yang M (2011). When MAGE meets RING: insights into biological functions of MAGE proteins. *Protein Cell* 2: 7-12.

Gaugler B, Van den Eynde B, van der Bruggen P, Romero P, Gaforio JJ, De Plaen E, Lethe B, Brasseur F, Boon T (1994). Human gene MAGE-3 codes for an antigen recognized on a melanoma by autologous cytolytic T lymphocytes. *J Exp Med* 179: 921-30.

Graff-Dubois S, Faure O, Gross DA, Alves P, Scardino A, Chouaib S, Lemonnier FA, Kosmatopoulos K (2002). Generation of CTL recognizing an HLA-A*0201-restricted epitope shared by MAGE-A1, -A2, -A3, -A4, -A6, -A10, and -A12 tumor antigens: implication in a broad-spectrum tumor immunotherapy. *J Immunol* 169: 575-80.

Harper JW, Adami GR, Wei N, Keyomarsi K, Elledge SJ (1993). The p21 Cdk-interacting protein Cip1 is a potent inhibitor of G1 cyclin-dependent kinases. *Cell* 75: 805-16.

Herin M, Lemoine C, Weynants P, Vessiere F, Van Pel A, Knuth A, Devos R, Boon T (1987). Production of stable cytolytic T-cell clones directed against autologous human melanoma. *Int J Cancer* 39: 390-6.

Itoh K, Hayashi A, Nakao M, Hoshino T, Seki N, Shichijo S (1996). Human tumor rejection antigens MAGE. *J Biochem* 119: 385-90.

Jang SJ, Soria JC, Wang L, Hassan KA, Morice RC, Walsh GL, Hong WK, Mao L (2001). Activation of melanoma antigen tumor antigens occurs early in lung carcinogenesis. *Cancer Res* 61: 7959-63.

Jordan BW, Dinev D, LeMellay V, Troppmair J, Gotz R, Wixler L, Sendtner M, Ludwig S, Rapp UR (2001). Neurotrophin receptor-interacting mage homologue is an

inducible inhibitor of apoptosis protein-interacting protein that augments cell death. *J Biol Chem* 276: 39985-9.

Kern SE, Kinzler KW, Bruskin A, Jarosz D, Friedman P, Prives C, Vogelstein B (1991). Identification of p53 as a sequence-specific DNA-binding protein. *Science* 252: 1708-11.

Kufer P, Zippelius A, Lutterbuse R, Mecklenburg I, Enzmann T, Montag A, Weckermann D, Passlick B, Prang N, Reichardt P, Dugas M, Kollermann MW, Pantel K, Riethmuller G (2002). Heterogeneous expression of MAGE-A genes in occult disseminated tumor cells: a novel multimarker reverse transcription-polymerase chain reaction for diagnosis of micrometastatic disease. *Cancer Res* 62: 251-61.

Laduron S, Deplus R, Zhou S, Kholmanskikh O, Godelaine D, De Smet C, Hayward SD, Fuks F, Boon T, De Plaen E (2004). MAGE-A1 interacts with adaptor SKIP and the deacetylase HDAC1 to repress transcription. *Nucleic Acids Res* 32: 4340-50.

Lee LG, Connell CR, Bloch W (1993). Allelic discrimination by nick-translation PCR with fluorogenic probes. *Nucleic Acids Res* 21: 3761-6.

Li H, Jeong YM, Kim SY, Kim MK, Kim DS (2011). Arbutin inhibits TCCSUP human bladder cancer cell proliferation via up-regulation of p21. *Pharmazie* 66: 306-9.

Lin J, Lin L, Thomas DG, Greenson JK, Giordano TJ, Robinson GS, Barve RA, Weishaar FA, Taylor JM, Orringer MB, Beer DG (2004). Melanoma-associated antigens in esophageal adenocarcinoma: identification of novel MAGE-A10 splice variants. *Clin Cancer Res* 10: 5708-16.

Livak KJ, Flood SJ, Marmaro J, Giusti W, Deetz K (1995). Oligonucleotides with fluorescent dyes at opposite ends provide a quenched probe system useful for detecting PCR product and nucleic acid hybridization. *PCR Methods Appl* 4: 357-62.

Livak KJ, Schmittgen TD (2001). Analysis of relative gene expression data using real-time quantitative PCR and the 2(-Delta Delta C(T)) Method. *Methods* 25: 402-8.

Lopez-Sanchez N, Gonzalez-Fernandez Z, Niinobe M, Yoshikawa K, Frade JM (2007). Single mage gene in the chicken genome encodes CMage, a protein with functional similarities to mammalian type II Mage proteins. *Physiol Genomics* 30: 156-71.

Lucas S, De Plaen E, Boon T (2000). MAGE-B5, MAGE-B6, MAGE-C2, and MAGE-C3: four new members of the MAGE family with tumor-specific expression. *Int J Cancer* 87: 55-60.

Lucas S, De Smet C, Arden KC, Viars CS, Lethe B, Lurquin C, Boon T (1998). Identification of a new MAGE gene with tumor-specific expression by representational difference analysis. *Cancer Res* 58: 743-52.

Lurquin C, De Smet C, Brasseur F, Muscatelli F, Martelange V, De Plaen E, Brasseur R, Monaco AP, Boon T (1997). Two members of the human MAGEB gene family located in Xp21.3 are expressed in tumors of various histological origins. *Genomics* 46: 397-408.

Masuda Y, Sasaki A, Shibuya H, Ueno N, Ikeda K, Watanabe K (2001). Dlxin-1, a novel protein that binds Dlx5 and regulates its transcriptional function. *J Biol Chem* 276: 5331-8.

Matlashewski G, Lamb P, Pim D, Peacock J, Crawford L, Benchimol S (1984). Isolation and characterization of a human p53 cDNA clone: expression of the human p53 gene. *EMBO J* 3: 3257-62.

Monte M, Simonatto M, Peche LY, Bublik DR, Gobessi S, Pierotti MA, Rodolfo M, Schneider C (2006). MAGE-A tumor antigens target p53 transactivation function through histone deacetylase recruitment and confer resistance to chemotherapeutic agents. *Proc Natl Acad Sci U S A* 103: 11160-5.

Mou DC, Cai SL, Peng JR, Wang Y, Chen HS, Pang XW, Leng XS, Chen WF (2002). Evaluation of MAGE-1 and MAGE-3 as tumour-specific markers to detect blood dissemination of hepatocellular carcinoma cells. *Br J Cancer* 86: 110-6.

Muscatelli F, Abrous DN, Massacrier A, Boccaccio I, Le Moal M, Cau P, Cremer H (2000). Disruption of the mouse Necdin gene results in hypothalamic and behavioral alterations reminiscent of the human Prader-Willi syndrome. *Hum Mol Genet* 9: 3101-10.

Muscatelli F, Walker AP, De Plaen E, Stafford AN, Monaco AP (1995). Isolation and characterization of a MAGE gene family in the Xp21.3 region. *Proc Natl Acad Sci U S A* 92: 4987-91.

Nagao T, Higashitsuji H, Nonoguchi K, Sakurai T, Dawson S, Mayer RJ, Itoh K, Fujita J (2003). MAGE-A4 interacts with the liver oncoprotein gankyrin and suppresses its tumorigenic activity. *J Biol Chem* 278: 10668-74.

Nardiello T, Jungbluth AA, Mei A, Diliberto M, Huang X, Dabrowski A, Andrade VC, Wasserstrum R, Ely S, Niesvizky R, Pearse R, Coleman M, Jayabalan DS, Bhardwaj N, Old LJ, Chen-Kiang S, Cho HJ (2011). MAGE-A inhibits apoptosis in proliferating myeloma cells through repression of Bax and maintenance of survivin. *Clin Cancer*

Res 17: 4309-19.

Niinobe M, Koyama K, Yoshikawa K (2000). Cellular and subcellular localization of necdin in fetal and adult mouse brain. *Dev Neurosci* 22: 310-9.

Nseyo UO, Lamm DL (1997). Immunotherapy of bladder cancer. *Semin Surg Oncol* 13: 342-9.

Ohman Forslund K, Nordqvist K (2001). The melanoma antigen genes--any clues to their functions in normal tissues? *Exp Cell Res* 265: 185-94.

Osterlund C, Tohonen V, Forslund KO, Nordqvist K (2000). Mage-b4, a novel melanoma antigen (MAGE) gene specifically expressed during germ cell differentiation. *Cancer Res* 60: 1054-61.

Otte M, Zafrakas M, Riethdorf L, Pichlmeier U, Loning T, Janicke F, Pantel K (2001). MAGE-A gene expression pattern in primary breast cancer. *Cancer Res* 61: 6682-7.

Paolella BR, Havrda MC, Mantani A, Wray CM, Zhang Z, Israel MA (2011). p53 directly represses Id2 to inhibit the proliferation of neural progenitor cells. *Stem Cells* 29: 1090-101.

Patton SE, Hall MC, Ozen H (2002). Bladder cancer. *Curr Opin Oncol* 14: 265-72.

Pei Y, Tuschl T (2006). On the art of identifying effective and specific siRNAs. *Nat Methods* 3: 670-6.

Peikert T, Specks U, Farver C, Erzurum SC, Comhair SA (2006). Melanoma antigen A4 is expressed in non-small cell lung cancers and promotes apoptosis. *Cancer Res* 66: 4693-700.

Ries J, Mollaoglu N, Toyoshima T, Vairaktaris E, Neukam FW, Ponader S, Nkenke E (2009). A novel multiple-marker method for the early diagnosis of oral squamous cell carcinoma. *Dis Markers* 27: 75-84.

Rimoldi D, Salvi S, Schultz-Thater E, Spagnoli GC, Cerottini JC (2000). Anti-MAGE-3 antibody 57B and anti-MAGE-1 antibody 6C1 can be used to study different proteins of the MAGE-A family. *Int J Cancer* 86: 749-51.

Rogner UC, Wilke K, Steck E, Korn B, Poustka A (1995). The melanoma antigen gene (MAGE) family is clustered in the chromosomal band Xq28. *Genomics* 29: 725-31.

Russo V, Lunghi F, Fontana R, Bregni M (2011). A Clinical Study of a Cell-Based

MAGE-A3 Active Immunotherapy in Advanced Melanoma Patients. *J Cancer* 2: 329-30.

Sakurai T, Itoh K, Higashitsuji H, Nagao T, Nonoguchi K, Chiba T, Fujita J (2004). A cleaved form of MAGE-A4 binds to Miz-1 and induces apoptosis in human cells. *J Biol Chem* 279: 15505-14.

Salehi AH, Roux PP, Kubu CJ, Zeindler C, Bhakar A, Tannis LL, Verdi JM, Barker PA (2000). NRAGE, a novel MAGE protein, interacts with the p75 neurotrophin receptor and facilitates nerve growth factor-dependent apoptosis. *Neuron* 27: 279-88.

Sang M, Lian Y, Zhou X, Shan B (2011a). MAGE-A family: attractive targets for cancer immunotherapy. *Vaccine* 29: 8496-500.

Sang M, Wang L, Ding C, Zhou X, Wang B, Lian Y, Shan B (2011b). Melanoma-associated antigen genes - an update. *Cancer Lett* 302: 85-90.

Sasaki M, Nakahira K, Kawano Y, Katakura H, Yoshimine T, Shimizu K, Kim SU, Ikenaka K (2001). MAGE-E1, a new member of the melanoma-associated antigen gene family and its expression in human glioma. *Cancer Res* 61: 4809-14.

Sharma P, Shen Y, Wen S, Bajorin DF, Reuter VE, Old LJ, Jungbluth AA (2006). Cancer-testis antigens: expression and correlation with survival in human urothelial carcinoma. *Clin Cancer Res* 12: 5442-7.

Simpson AJ, Caballero OL, Jungbluth A, Chen YT, Old LJ (2005). Cancer/testis antigens, gametogenesis and cancer. *Nat Rev Cancer* 5: 615-25.

Suyama T, Ohashi H, Nagai H, Hatano S, Asano H, Murate T, Saito H, Kinoshita T (2002). The MAGE-A1 gene expression is not determined solely by methylation status of the promoter region in hematological malignancies. *Leuk Res* 26: 1113-8.

Taback B, Chan AD, Kuo CT, Bostick PJ, Wang HJ, Giuliano AE, Hoon DS (2001). Detection of occult metastatic breast cancer cells in blood by a multimolecular marker assay: correlation with clinical stage of disease. *Cancer Res* 61: 8845-50.

Taniura H, Matsumoto K, Yoshikawa K (1999). Physical and functional interactions of neuronal growth suppressor necdin with p53. *J Biol Chem* 274: 16242-8.

Taniura H, Taniguchi N, Hara M, Yoshikawa K (1998). Necdin, a postmitotic neuron-specific growth suppressor, interacts with viral transforming proteins and cellular transcription factor E2F1. *J Biol Chem* 273: 720-8.

Traversari C, van der Bruggen P, Luescher IF, Lurquin C, Chomez P, Van Pel A, De

Plaen E, Amar-Costesec A, Boon T (1992a). A nonapeptide encoded by human gene MAGE-1 is recognized on HLA-A1 by cytolytic T lymphocytes directed against tumor antigen MZ2-E. *J Exp Med* 176: 1453-7.

Traversari C, van der Bruggen P, Van den Eynde B, Hainaut P, Lemoine C, Ohta N, Old L, Boon T (1992b). Transfection and expression of a gene coding for a human melanoma antigen recognized by autologous cytolytic T lymphocytes. *Immunogenetics* 35: 145-52.

Tyagi P, Mirakhur B (2009). MAGRIT: the largest-ever phase III lung cancer trial aims to establish a novel tumor-specific approach to therapy. *Clin Lung Cancer* 10: 371-4.

van der Bruggen P, Traversari C, Chomez P, Lurquin C, De Plaen E, Van den Eynde B, Knuth A, Boon T (1991). A gene encoding an antigen recognized by cytolytic T lymphocytes on a human melanoma. *Science* 254: 1643-7.

Wang TS, Ding QQ, Guo RH, Shen H, Sun J, Lu KH, You SH, Ge HM, Shu YQ, Liu P (2010). Expression of livin in gastric cancer and induction of apoptosis in SGC-7901 cells by shRNA-mediated silencing of livin gene. *Biomed Pharmacother* 64: 333-8.

Xia LP, Xu M, Chen Y, Shao WW (2012). Expression of MAGE-A11 in breast cancer tissues and its effects on the proliferation of breast cancer cells. *Mol Med Report*.

Yang B, O'Herrin SM, Wu J, Reagan-Shaw S, Ma Y, Bhat KM, Gravekamp C, Setaluri V, Peters N, Hoffmann FM, Peng H, Ivanov AV, Simpson AJ, Longley BJ (2007). MAGE-A, mMage-b, and MAGE-C proteins form complexes with KAP1 and suppress p53-dependent apoptosis in MAGE-positive cell lines. *Cancer Res* 67: 9954-62.

Yang D, Song X, Zhang J, Ye L, Wang S, Che X, Wang J, Zhang Z, Wang L (2010). Suppression of livin gene expression by siRNA leads to growth inhibition and apoptosis induction in human bladder cancer T24 cells. *Biosci Biotechnol Biochem* 74: 1039-44.

Yin B, Liu G, Wang XS, Zhang H, Song YS, Wu B (2011). Expression profile of cancer-testis genes in transitional cell carcinoma of the bladder. *Urol Oncol*.

Zendman AJ, Ruiter DJ, Van Muijen GN (2003). Cancer/testis-associated genes: identification, expression profile, and putative function. *J Cell Physiol* 194: 272-88.

Zhu X, Asa SL, Ezzat S (2008). Fibroblast growth factor 2 and estrogen control the balance of histone 3 modifications targeting MAGE-A3 in pituitary neoplasia. *Clin*

Cancer Res 14: 1984-96.

8. Acknowledgments

First of all, I want to show my great appreciation to my supervisor, **PD Dr. Jörg Hänze**, for his enthusiastic support, patient education, constructive comments, intensive theoretical discussions and intellectual guidance that he extended to me throughout my study. I also deeply appreciate his correction and critical comments in reviewing and revising the manuscript of this thesis and continuous encouragement throughout my study saving no effort.

I also want to express my sincere gratitude to **PD Dr. med. Peter J. Olbert** and **Prof. Dr. Rainer Hofmann** who gave me the precious opportunity to do my study at the Faculty of Medicine of Philipps-University Marburg and deeply thank them for their supports and kindly help during my study.

My special thanks should go to **Kati Oplesch, Nadine Zimmer, Helga Kirchner, Anna Boide** and **Min Zhao** for their excellent technical supports in the laboratory and wonderful suggestions on my thesis writing.

I am very much obliged to **Prof. Dr. Jörg Bartsch** for his warm assistance and endless solicitude. It is him who taught me the meaning of "Always in the mood".

I am extremely grateful to **Ping Huang** who inspires me and makes me happy all the time, especially when I am depressed. Thank her for supporting me spiritually.

I am indebted to my dear parents, my brother **Wenjun Zhou** and family members for their loving, understanding, encouragement and support through all these years.

Last but not least, I would like to express my heartfelt thanks to my beloved wife **Fangyong Dong**, my son **Xuanqi Zhou** and **Hongting Zhou**, for their endless love,

sustained encouragement and company throughout my life. I could not have succeeded without their support.

This dissertation, and the doctor title, are the rewards for all the people who love me and help me on the way. They are also a gift for my father in the heaven, who is the mentor of my life and soul.